Inorg. Chem. **2008**, *47*, 6931−6947

Copper(I) Cyanide Networks: Synthesis, Structure, and Luminescence Behavior. Part 2. Piperazine Ligands and Hexamethylenetetramine[1]

Mi Jung Lim, Courtney A. Murray, Tristan A. Tronic, Kathryn E. deKrafft, Amanda N. Ley, Jordan C. deButts, Robert D. Pike,* Haiyan Lu, and Howard H. Patterson*

Department of Chemistry, College of William and Mary, Williamsburg, Virginia 23187-8795, and Department of Chemistry, University of Maine, Orono, Maine 04469-5706

Received March 21, 2008

A variety of photoluminescent, and in some cases thermochromic, metal−organic networks of CuCN were self-assembled in aqueous reactions with amine ligands: $(CuCN)_2$(Pip) (**1a**), $(CuCN)_{20}(Pip)_7$ (**1b**), $(CuCN)_7(MePip)_2$ (**2**), $(CuCN)_2(Me_2Pip)$ (**3a**), $(CuCN)_4(Me_2Pip)$ (**3b**), $(CuCN)_7(EtPip)_2$ (**4**), $(CuCN)_4(Et_2Pip)$ (**5**), $(CuCN)_3(BzPip)_2$ (**6a**), $(CuCN)_5(BzPip)_2$ (**6b**), $(CuCN)_7(BzPip)_2$ (**6c**), $(CuCN)_4$(BzPip) (**6d**), $(CuCN)_2(Bz_2Pip)$ (**7**), (CuCN)(Ph_2CHPip) (**8a**), $(CuCN)_2(Ph_2CHPip)$ (**8b**), $(CuCN)_3(HMTA)_2$ (**9a**), $(CuCN)_5(HMTA)_2$ (**9b**), and $(CuCN)_5$(HMTA) (**9c**) (Pip = piperazine, MePip = *N*-methylpiperazine, Me_2Pip = *N*,*N*′-dimethylpiperazine, EtPip = *N*-ethylpiperazine, Et_2Pip = *N*,*N*′-diethylpiperazine, BzPip = *N*-benzylpiperazine, Bz_2Pip = *N*,*N*′-dibenzylpiperazine, Ph_2CHPip = *N*-(diphenylmethyl)piperazine, and HMTA = hexamethylenetetramine). New X-ray structures are reported for **1b**, **2**, **3b**, **4**, **5**, **6a**, **6d**, **7**, **8b**, **9b**, and **9c**. An important structural theme is the formation of (6,3) $(CuCN)_2$(piperazine) sheets with or without threading of independent CuCN chains. Strong luminescence at ambient temperature is observed for all but complexes **6** and **7**. All luminescent compounds show a broad emission band in the blue region at about 450 nm attributable to metal-to-ligand charge transfer behavior based on the large Stokes shift between excitation and emission maxima. **3**, **8**, and **9** are thermochromic due to an additional lower energy emission band, which is absent at 77 K.

Introduction

We are currently studying the extensive metal−organic network chemistry of copper(I) cyanide with bridging nitrogen ligands (L).[1−3] Because a single cyanide ligand can bridge two, three, or even four metal centers, it serves as an excellent network former. Porous networks have potential applications in areas such as separations, gas storage, and catalysis.[4] In addition, highly luminescent metal−organic materials might be used in sensing systems when molecular absorption of small molecules leads to an alteration in network luminescence behavior.[5] Our recent work has shown that diimine L networks of CuCN are at best weakly luminescent.[1] In the current study, we report the network formation and luminescence behavior of CuCN with diamine and tetramine ligands, in particular substituted piperazines and hexamethylenetetramine (HMTA), as in Chart 1. Many of the resulting networks are intensely luminescent.[2] The relationship between structure and luminescence is examined herein. Some of this work has been previously communicated.[2]

Chart 1

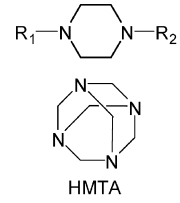

Pip: R_1, R_2 = H
MePip: R_1 = H, R_2 = CH_3
Me_2Pip: R_1, R_2 = CH_3
EtPip: R_1 = H, R_2 = CH_2CH_3
Et_2Pip: R_1, R_2 = CH_2CH_3
PhPip: R_1 = H, R_2 = C_6H_5
BzPip: R_1 = H, R_2 = $CH_2C_6H_5$
Bz_2Pip: R_1, R_2 = $CH_2C_6H_5$
Ph_2CHPip: R_1 = H, R_2 = $CH(C_6H_5)_2$

In contrast to studies of diimine L with CuCN,[1,3,6] relatively few diamine ligands have been used to extend the CuCN network. Known networks are limited to the following: $(CuCN)_2$L (L = Pip, Me_2Pip, 1,4-butanediamine, and *N*,*N*,*N*′,*N*′-tetramethylethylenediamine), and (CuCN)(N-phenylpiperazine),[7] as well as the tetramine complex

* To whom correspondence should be addressed. E-mail: rdpike@wm.edu, Tel: 757-2212555, Fax: 757-2212715 (R.D.P.); E-mail: howardp@maine.edu, Tel: 207-5811178, Fax: 207-5811191 (H.H.P.).

(1) Tronic, T. A.; deKrafft, K. E.; Lim, M. J.; Ley, A. N.; Pike, R. D. *Inorg. Chem.* **2007**, *46*, 8897.
(2) Pike, R. D.; deKrafft, K. E.; Ley, A. N.; Tronic, T. A. *Chem. Commun.* **2007**, 3732.
(3) Pagola, S.; Pike, R. D.; deKrafft, K. E.; Tronic, T. A. *Acta Crystallogr., Sect. C* **2008**, *64*, m132.

10.1021/ic8005184 CCC: $40.75
Published on Web 07/02/2008

$(CuCN)_3(HMTA)_2$, in which HMTA behaves in a bidentate fashion.[8] In addition to the relative paucity of reported diamine-CuCN networks is the fact that only 1:1, 3:2, and 2:1 CuCN/L stoichiometries have been encountered thus far. Each of the known $(CuCN)_2L$ materials exhibits a simple network of CuCN chains cross-linked by L. This produces hexagonally tiled 2D sheets with 3-coordinate copper centers, best described as a (6,3) network.[9] Given the diverse array of copper-rich networks identified for diimine L having CuCN/L ratios as high as 4:1,[1,6] it seemed likely that a variety of copper-rich products would also be found using piperazines and HMTA.

Experimental Section

Materials and Methods. All reagents were purchased from Aldrich or Acros and used without purification, except for BzPip and Bz_2Pip, which were prepared as described below. All water used was ultrafiltered deionized quality and was thoroughly degassed with argon. Analyses for carbon, hydrogen, and nitrogen were carried out by Atlantic Microlabs, Norcross, GA. Ambient temperature-luminescence measurements were carried out on well-ground powders using a PerkinElmer LS 55 spectrofluorimeter. Steady-state photoluminescence at ambient and reduced temperature were collected using a Photon Technology International Model Quanta-Master-1046 spectrophotometer equipped with a 75 W xenon lamp. Wavelengths were selected with two excitation monochromators and a single emission monochromator. A model LT-3−110-Heli-Trans cryogenic liquid transfer system equipped with a temperature controller was used to record luminescence spectra as a function of temperature. IR measurements were made on KBr pellets using a Digilab FTS 7000 FTIR spectrophotometer. Thermogravimetric analyses (TGA) were conducted using a TA Instruments Q500 in the dynamic (variable temperature) mode with a maximum heating rate of 50 °C/min to 900 °C under 60 mL/min N_2 flow.

Ligand Syntheses. BzPip.[10] A solution of benzyl chloride (10.0 g, 79.0 mmol) and Pip (27.2 g, 316 mmol) in 250 mL toluene was heated to 85 °C for 2 h. The resulting yellow solution was filtered and evaporated. The oily residue was extracted with 2 M HCl and CH_2Cl_2 (50 mL each). The aqueous fraction was then basified to ca. pH 14 with solid NaOH. It was then re-extracted with CH_2Cl_2 (2×100 mL). The organic layer was washed with brine and water and then dried over anhydrous Na_2SO_4. Evaporation left a colorless oil which was dried in vacuo (8.97 g, 50.9 mmol, 64.4%). ^1H NMR (400 MHz, $CDCl_3$) δ 7.30 (m, 5H, Ph), 3.49 (s, 2H, CH_2Ph), 2.88 (m, 2H CH_2), 2.41 (br s, 2H, CH_2), 1.61 (br s, 1H, NH). $^{13}C\{^1H\}$ NMR (100 MHz, $CDCl_3$) δ 138.22, 129.31, 128.31, 127.12, 63.91, 54.73, 46.34.

Bz_2Pip.[11] Solutions of Pip (0.315 g, 3.66 mmol) and freshly distilled benzaldehyde (64.6 g, 6.09 mmol) dissolved in separate 10 mL portions of CH_2Cl_2 were combined, forming a clear, colorless solution. Solid $NaBH(OAc)_3$ (1.27 g, 5.97 mmol) was added, and the resulting suspension was stirred for 4 h under N_2. The mixture was washed with saturated aq $NaHCO_3$ (20 mL), and the aqueous layer was re-extracted three times with 25 mL CH_2Cl_2. The organic layers were combined and dried over anhydrous Na_2SO_4. Evaporation left a white solid that was dried in vacuo (0.398 g, 49.1%). ^1H NMR (400 MHz, $CDCl_3$) δ 7.30 (m, 10H, Ph), 3.51 (s, 4H, CH_2Ph), 2.48 (s, 8H, CH_2CH_2). $^{13}C\{^1H\}$ NMR (100 MHz, $CDCl_3$) δ 138.21, 129.56, 128.48, 127.33, 63.39, 53.35.

Network Syntheses. $(CuCN)_2(Pip)$, 1a. Copper(I) cyanide (0.268 g, 3.00 mmol) and KCN (0.130 g, 2.00 mmol) were suspended in 20 mL H_2O. The mixture was heated under N_2 and Pip (0.0861 g, 1.00 mmol) was added. The suspension was vigorously stirred at about 80 °C for 1 h. The suspended solid was collected by means of filtration, washed with H_2O, ethanol, and diethyl ether, and then dried under vacuum. A pale-yellow powder was isolated (1.37 g, 5.16 mmol, 51.6%). IR (KBr pellet, cm^{-1}) 3244 (w), 3153 (w), 3101 (m), 3038 (m), 2104 (s), 1575 (m), 1439 (m), 1405 (m), 1382 (m), 1103 (m), 990 (w), 968 (m), 867 (m). Anal. Calcd for $C_6H_{10}N_4Cu_2$: C, 27.17; H, 3.80; N, 21.12. Found: C, 27.48; H, 3.85; N, 21.73. TGA Calcd for CuCN: 67.5. Found: 68.0 (175−245 °C).

$(CuCN)_{20}(Pip)_7$, 1b.[2] The procedure was identical to that used for **1a**, using 4.00 mmol CuCN, 2.00 mmol KCN, and 1.00 mmol Pip. A cream powder was isolated (85.1%). IR (KBr pellet, cm^{-1}) 3246 (m), 2990 (w), 2911 (m), 2881 (m), 2857 (m), 2124 (s), 1449 (m), 1311 (s), 1277 (w), 1115 (m), 1099 (s), 990 (w), 870 (s), 624 (w). Anal. Calcd for $C_{48}H_{70}N_{34}Cu_{20}$: C, 24.08; H, 2.95; N 19.89. Found: C, 24.27; H, 2.97; N, 20.05. TGA Calcd for CuCN: 74.8. Found: 74.9 (185−240 °C).

$(CuCN)_7(MePip)_2$, 2. The procedure was identical to that used for **1a**, using 4.00 mmol CuCN, 2.00 mmol KCN, and 1.00 mmol MePip. A white powder was isolated (63.0%). IR (KBr pellet, cm^{-1}) 3296 (m), 3233 (w), 2951 (w), 2866 (w), 2837 (m), 2819 (w), 2156 (m), 2145 (m), 2122 (s), 1450 (m), 1311 (m), 1283 (s), 1261 (w), 1125 (m), 1055 (w), 1032 (w), 1003 (m), 973 (w), 944 (w) 860 (s), 779 (w), 625 (w). Anal. Calcd for $C_{17}H_{24}N_{11}Cu_7$: C, 24.68; H, 2.92; N, 18.62. Found: C, 24.48; H, 2.88; N, 18.70. TGA Calcd for CuCN: 75.9 Found 76.6 (175−230 °C).

(4) (a) Muller, U.; Schubert, M.; Teich, F.; Puetter, H.; Schierle-Arndt, K.; Pastré, J. *J. Mater. Chem.* **2006**, *16*, 626. (b) Dincă, M.; Yu, A. F.; Long, J. R. *J. Am. Chem. Soc.* **2006**, *128*, 8904. (c) Rowsell, J. L. C.; Yaghi, O. M. *J. Am. Chem. Soc.* **2006**, *128*, 1304. (d) Forster, P. M.; Cheetham, A. K. *Top. Catal.* **2003**, *24*, 79. (e) Kesanli, B.; Lin, W. *Coord. Chem. Rev.* **2003**, *246*, 305.

(5) (a) Exstrom, C. L.; Sowa, J. L., Jr.; Daws, C. A.; Janzen, D.; Mann, K. R.; Moore, G. A.; Stewart, F. F. *Chem. Mater.* **1995**, *7*, 15. (b) Daws, C. A.; Exstrom, C. L.; Sowa, J. L., Jr.; Mann, K. R. *Chem. Mater.* **1997**, *9*, 363. (c) Vickery, J. C.; Olmstead, M. M.; Fung, E. Y.; Balch, A. L. *Angew. Chem, Int. Ed.* **1997**, *36*, 1179. (d) Cariati, E.; Bu, X.; Ford, P. C. *Chem. Mater.* **2000**, *12*, 3385. (e) Drew, S. M.; Janzen, D. E.; Buss, C. E.; MacEwen, D. I.; Dublin, K. I.; Mann, K. R. *J. Am. Chem. Soc.* **2001**, *123*, 8414. (f) Buss, C. E.; Mann, K. R. *J. Am. Chem. Soc.* **2002**, *124*, 1031. (g) Fernández, E. J.; López-de-Luzuriaga, J. M.; Monge, M.; Olmos, M. E.; Pérez, J.; Laguna, A.; Mohamed, A. A.; Fackler, J. P., Jr. *J. Am. Chem. Soc.* **2003**, *125*, 2022. (h) Lu, W.; Chan, M. C. W.; Zhu, N.; Che, C.-M.; He, Z.; Wong, K.-Y. *Chem.—Eur. J.* **2003**, *9*, 6155.

(6) (a) Cromer, D. T.; Larson, A. C. *Acta Crystallogr., Sect. B* **1972**, *28*, 1052. (b) Chesnut, D. J.; Kusnetzow, A.; Zubieta, J. *J. Chem. Soc., Dalton Trans.* **1998**, 4081. (c) Teichert, O.; Sheldrick, W. S. *Z. Anorg. Allg. Chem.* **1999**, *625*, 1860. (d) Kuhlman, R.; Schimek, G. L.; Kolis, J. W. *Polyhedron* **1999**, *18*, 1379. (e) Teichert, O.; Sheldrick, W. S. *Z. Anorg. Allg. Chem.* **2000**, *626*, 1509. (f) Chesnut, D. J.; Plewak, D.; Zubieta, J. *J. Chem. Soc., Dalton Trans.* **2001**, 2567. (g) Hanika-Heidl, H.; Etaiw, S. E. H.; Ibrahim, M. S.; El-din, A. S. B.; Fischer, R. D. *J. Organomet. Chem.* **2003**, *684*, 329. (h) Greve, J.; Näther, C. *Z. Naturforsch.* **2004**, *59b*, 1325. (i) Hibble, S. J.; Chippindale, A. M. *Z. Anorg. Allg. Chem.* **2005**, *631*, 542. (j) Jess, I.; Näther, C. *Acta Crystallogr., Sect. E* **2006**, *62*, m721. (k) Lin, J.-D.; Li, Z.-H.; Li, T.; Li, J.-R.; Du, S.-W. *Inorg. Chem. Commun.* **2006**, *6*, 675.

(7) Stocker, F. B.; Staeva, T. P.; Rienstra, C. M.; Britton, D. *Inorg. Chem.* **1999**, *38*, 984.

(8) Stocker, F. B. *Inorg. Chem.* **1991**, *30*, 1472.

(9) Batten, S. R.; Robson, R. *Angew. Chem., Int. Ed.* **1998**, *37*, 1460.

(10) Capuano, B.; Crosby, I. T.; Lloyd, E. J.; Taylor, D. A. *Aust. J. Chem.* **2002**, *55*, 565.

(11) Denmark, S. E.; Fu, J. *Org. Lett.* **2002**, *4*, 1951.

$(CuCN)_2(Me_2Pip)$, 3a. The procedure was identical to that used for **1a**, using 3.00 mmol CuCN, 2.00 mmol KCN, and 1.00 mmol Me_2Pip. A white powder was isolated (52.7%). IR (KBr pellet, cm^{-1}) 2968 (m), 2826 (m), 2816 (m), 2135 (s), 1456 (s), 1290 (m), 1165 (m), 1123 (w), 1095 (w), 1049 (w), 1011 (s), 907 (w), 814 (w). Anal. Calcd for $C_8H_{14}N_4Cu_2$: C, 32.76; H, 4.81; N, 19.10. Found: C, 32.94; H, 4.91; N, 19.19. TGA Calcd for $(CuCN)_4(Me_2Pip)$: 80.5 (135−175 °C). Found: 80.7 (175−215 °C). Calcd for CuCN: 61.1. Found: 62.0 (180−215 °C).

$(CuCN)_4(Me_2Pip)$, 3b. The procedure was identical to that used for **1a**, using 4.00 mmol CuCN, 2.00 mmol KCN, and 1.00 mmol Me_2Pip. A white powder was isolated (59.1%). IR (KBr pellet, cm^{-1}) 2974 (m), 2947 (w), 2832 (m), 2820 (m), 2149 (m), 2127 (s), 1453 (s), 1367 (w), 1284 (s), 1151 (m), 1119 (m), 1089 (m), 1037 (m), 1005 (s), 910 (w), 817 (s), 633 (w). Anal. Calcd for $C_{10}H_{14}N_6Cu_4$: C, 25.42; H, 2.99; N, 17.79. Found: C, 25.65; H, 3.01; N, 17.94. TGA Calcd for CuCN: 75.8. Found: 76.1 (180−220 °C).

$(CuCN)_7(EtPip)_2$, 4. The procedure was identical to that used for **1a**, using 4.00 mmol CuCN, 2.00 mmol KCN, and 1.00 mmol EtPip. A white powder was isolated (65.7%). IR (KBr pellet, cm^{-1}) 3286 (w), 3236 (w), 2974 (w), 2836 (m), 2145 (m), 2120 (s), 1444 (w), 1315 (w), 1225 (m), 1094 (m), 1028 (w), 930 (m), 856 (m), 964 (w), 771 (w), 625 (w). Anal. Calcd for $C_{19}H_{28}N_{11}Cu_7$: C, 26.68; H, 3.30; N, 18.01. Found: C, 27.38; H, 3.32; N, 17.72. TGA Calcd for CuCN: 73.3. Found: 72.0 (180−230 °C).

$(CuCN)_4(Et_2Pip)$, 5. The procedure was identical to that used for **1a**, using 5.00 mmol CuCN, 3.00 mmol KCN, and 1.00 mmol Et_2Pip. A white powder was isolated (89.0%). IR (KBr pellet, cm^{-1}) 2970 (m), 2928 (w), 2900 (w), 2879 (w), 2839 (m), 2152 (m), 2119 (s), 1462 (w), 1445 (w), 1380 (w), 1316 (w), 1269 (w), 1142 (m), 1103 (m), 1018 (m), 941 (m), 831 (w), 784 (w). Anal. Calcd for $C_{12}H_{18}N_6Cu_4$: C, 28.80; H, 3.62; N, 16.79. Found: C, 28.76; H, 3.63; N, 16.81. TGA Calcd for CuCN: 73.3. Found: 72.1 (205−245 °C).

$(CuCN)_3(BzPip)_2$, 6a. The procedure was identical to that used for **1a**, using 2.00 mmol CuCN, 2.00 mmol KCN, and 1.00 mmol BzPip. A pale yellow powder was isolated (40.3%). IR (KBr pellet, cm^{-1}) 3285 (m), 3326 (w), 3027 (w), 2957 (m), 2853 (m), 2809 (m), 2124 (s), 2111 (s), 1491 (w), 1452 (m) 1339 (w), 1316 (m), 1119 (m), 1071 (w), 989 (w), 862 (m), 746 (m), 701 (m). Anal. Calcd for $C_{25}H_{32}N_7Cu_3$: C, 48.34; H, 5.19; N, 15.78. Found: C, 48.36; H, 5.13; N, 15.79. TGA Calcd for $(CuCN)_3$(BzPip): 71.6. Found: 72.4 (125−155 °C). Calcd for CuCN: 43.3. Found: 43.5 (155−220 °C).

$(CuCN)_5(BzPip)_2$, 6b. The procedure was identical to that used for **1a**, using 3.00 mmol CuCN, 2.00 mmol KCN, and 1.00 mmol BzPip. A cream powder was isolated (58.6%). IR (KBr pellet, cm^{-1}) 3282 (w), 3250 (w), 3026 (w), 2925 (w), 2893 (w), 2841 (m), 2161 (m), 2127 (s), 1491 (w), 1451 (m), 1315 (w), 1159 (w), 1101 (m), 987 (w), 965 (m), 862 (m), 745 (m), 702 (m). Anal. Calcd for $C_{27}H_{32}N_9Cu_5$: C, 40.52; H, 4.03; N, 15.75. Found: C, 41.04; H, 4.16; N, 15.77. TGA Calcd for $(CuCN)_4$(BzPip): 83.5. Found: 83.7 (125−145 °C). Calcd for CuCN: 56.0. Found: 55.9 (145−200 °C).

$(CuCN)_7(BzPip)_2$, 6c. The procedure was identical to that used for **1a**, using 4.00 mmol CuCN, 2.00 mmol KCN, and 1.00 mmol BzPip. An off-white powder was isolated (72.8%). IR (KBr pellet, cm^{-1}) 3246 (m), 3024 (w), 2926 (m), 2835 (m), 2811 (m), 2162 (m), 2128 (s), 2123 (s), 2090 (s) 1490 (w), 1439 (m), 1161 (w), 1095 (m), 1022 (w), 984 (m), 962 (m), 742 (s), 700 (s). Anal. Calcd for $C_{29}H_{32}N_{11}Cu_7$: C, 35.56; H, 3.29; N, 15.73. Found: C, 35.87; H, 3.36; N, 15.53. TGA Calcd for CuCN: 64.0. Found: 63.4 (140−220 °C).

$(CuCN)_4$(BzPip), 6d. The procedure was identical to that used for **1a**, using 5.00 mmol CuCN, 3.00 mmol KCN, and 1.00 mmol BzPip. An off-white powder was isolated (70.5%). IR (KBr pellet, cm^{-1}) 3026 (w), 2971 (w), 2930 (w), 2836 (m), 2162 (s), 2119 (s), 1446 (m), 1167 (m), 1096 (m), 961 (s), 857 (m), 768 (m), 745 (m), 702 (s). Anal. Calcd for $C_{15}H_{16}N_6Cu_4$: C, 33.71; H, 3.02; N, 15.72. Found: C, 33.22; H, 2.98; N, 15.64. TGA Calcd for CuCN: 67.0. Found: 67.8 (145−215 °C).

$(CuCN)_2(Bz_2Pip)$, 7. The procedure was identical to that used for **1a**, using 2.00 mmol CuCN, 2.00 mmol KCN, and 1.00 mmol Bz_2Pip. A light-tan powder was isolated (33.0%). IR (KBr pellet, cm^{-1}) 3061 (w), 3026 (w), 2967 (w), 2874 (w), 2832 (m), 2805 (m) 2126 (s), 1492 (w), 1451 (s), 1399 (m), 1345 (m), 1265 (m), 1130 (m), 1114 (m), 997 (m), 937 (m), 833 (m), 754 (s), 702 (s). Anal. Calcd for $C_{20}H_{22}N_4Cu_2$: C, 53.92; H, 4.98; N, 12.58. Found: C, 53.87; H, 4.98; N, 12.50. TGA Calcd for CuCN: 40.2. Found: 40.6 (180−215 °C).

$(CuCN)(Ph_2CHPip)$, 8a. The procedure was identical to that used for **1a**, using 2.00 mmol CuCN, 2.00 mmol KCN, and 1.00 mmol Ph_2CHPip. A white powder was isolated (36.4%). IR (KBr pellet, cm^{-1}) 3059 (w), 3026 (w), 2960 (m), 2850 (w), 2802 (w), 2134 (s), 2130 (s), 1490 (m), 1450 (m), 1318 (w), 1123 (m), 1072 (w), 1006 (w), 920 (w), 869 (s), 751 (s), 702 (s). Anal. Calcd for $C_{18}H_{20}N_3Cu$: C, 63.23; H, 5.90; N, 12.29. Found: C, 62.96; H, 5.83; N, 12.43. TGA Calcd for $(CuCN)_2(Ph_2CHPip)$: 63.1. Found: 63.3 (150−185 °C). Calcd for CuCN: 26.2. Found: 26.6 (185−215 °C).

$(CuCN)_2(Ph_2CHPip)$, 8b. The procedure was identical to that used for **1a**, using 3.00 mmol CuCN, 2.00 mmol KCN, and 1.00 mmol Ph_2CHPip. A white powder was isolated (67.4%). IR (KBr pellet, cm^{-1}) 3265 (w), 3026 (w), 2972 (w), 2808 (w), 2768 (w), 2738 (w), 2127 (s), 1490 (m), 1449 (s), 1342 (w), 1310 (m), 1129 (m), 1072 (m), 1007 (m), 851 (m), 752 (m), 706 (s). Anal. Calcd for $C_{19}H_{20}N_4Cu_2$: C, 52.89; H, 4.67; N, 12.98. Found: C, 53.57; H, 4.66; N, 12.65. TGA Calcd for CuCN: 41.5. Found: 41.6 (145−240 °C).

$(CuCN)_3(HMTA)_2$, 9a. The procedure was identical to that used for **1a**, using 1.00 mmol CuCN, 1.00 mmol KCN and 1.00 mmol HMTA. A white powder was isolated (30.0%). IR (KBr pellet, cm^{-1}) 2956 (w), 2945 (w), 2920 (w), 2875 (w), 2132 (m), 2114 (m), 1460 (m), 1368 (w), 1243 (m), 1231 (m), 1222 (m), 1048 (m), 1020 (m), 990 (s), 829 (m), 820 (m), 802 (m), 783 (w), 708 (m), 683 (m), 662 (m). Anal. Calcd for $C_{15}H_{24}N_{11}Cu_3$: C, 32.81; H, 4.41; N, 28.06. Found: C, 32.87; H, 4.39; N, 28.06. TGA Calcd for $(CuCN)_5$(HMTA): 64.3. Found: 64.5 (215−270 °C). Calcd for CuCN: 48.9. Found: 49.6 (290−335 °C).

$(CuCN)_5(HMTA)_2$, 9b. The procedure was identical to that used for **1a**, using 2.00 mmol CuCN, 2.00 mmol KCN, and 1.00 mmol HMTA and heating for 5 h. A white powder was isolated (39.7%). IR (KBr pellet, cm^{-1}) 2995 (w), 2990 (w), 2956 (w), 2930 (w), 2881 (w), 2108 (m), 2098 (m), 2088 (m), 2072 (m), 1454 (m), 1366 (w), 1238 (s), 1223 (s), 1062 (m), 1026 (s), 1006 (s), 989 (s), 928 (w), 841 (m), 808 (m), 701 (m), 670 (m). Anal. Calcd for $C_{17}H_{24}N_{13}Cu_5$: C, 28.04; H, 3.32; N, 25.01. Found: C, 28.32; H, 3.41; N, 25.19. TGA Calcd for $(CuCN)_5$(HMTA): 80.7. Found: 81.8 (240−270 °C). Calcd for CuCN: 61.5. Found: 63.7 (270−330 °C).

$(CuCN)_5$(HMTA), 9c. The procedure was identical to that used for **1a**, using 4.00 mmol CuCN, 2.00 mmol KCN, and 1.00 mmol HMTA. A white powder was isolated (59.1%). IR (KBr pellet, cm^{-1}) 2950 (w), 2158 (w), 2148 (w), 2106 (w), 2080 (m), 1462 (w), 1236 (m), 1003 (s), 827 (m), 810 (m), 707 (w), 700 (m), 689 (w). Anal. Calcd for $C_{11}H_{12}N_9Cu_5$: C, 22.47; H, 2.06; N, 21.44. Found: C, 22.65; H, 2.07; N, 21.47. TGA Calcd for CuCN: 76.2. Found: 77.8 (290−330 °C).

General Method for Hydrothermal (HT) Reactions. Copper(I) cyanide and KCN were suspended in 5.0 mL H_2O in a 23 mL Teflon-lined Parr acid digestion vessel. The L ligand was added, and the resulting suspension was stirred briefly. The vessel was sealed and heated at 175 °C for 4 days. After overnight cooling to room temperature, the suspended solid was collected by means of filtration, washed with H_2O, ethanol, and diethyl ether, and then dried under vacuum. Crystals of sufficient quality for X-ray analysis were then selected. The following mmol ratios of CuCN/KCN/L were used to produce X-ray crystals: **1b** (3:1:1), **2** (2:1:1), **3b** (4:1:1), **4** (2:1:1), **5** (2:1:1), **6a** (1:1:1), **6d** (2:1:1), **7** (2:1:1), **8b** (4:1:1), **9b** (4:1:1), and **9c** (5:2:1).

X-ray Analysis. Single-crystal determinations were carried out using a Bruker *SMART Apex II* diffractometer using graphite-monochromated Cu Kα radiation.[12] The data were corrected for Lorentz and polarization[13] effects and absorption using *SADABS*.[14] The structures were solved by use of direct methods or Patterson map. Least squares refinement on F^2 was used for all reflections. Structure solution, refinement, and the calculation of derived results were performed using the *SHELXTL*[15] software package. The non-hydrogen atoms were refined anisotropically with one exception. The (ordered) cyano atom C5 in **9c** could not successfully be made anisotropic despite attempts to model it in multiple positions and despite removal of several offending reflections. For **2** and **3b**, hydrogen atoms were located by standard difference Fourier techniques and were refined with isotropic thermal parameters. In all other cases, hydrogen atoms were located and then placed in theoretical positions. In most, but not all cases, the cyano carbon and nitrogen atoms were disordered. When required by crystallographic symmetry, occupancies of 50% carbon and 50% nitrogen were used; otherwise relative carbon and nitrogen occupancies were refined. The former and latter cases are referred to in the text as symmetrically and non-symmetrically disordered, respectively. All ethyl groups in **4** and **5** were disordered across mirror planes. This disorder was successfully modeled.

Powder-diffraction analysis was carried out on the instrument described above. Samples were ground and prepared as mulls using Paratone-N oil. Four 180 s frames were collected, covering 8−100° 2θ. Frames were merged using the *SMART Apex II* software[12] and were further processed using *DIFFRAC-Plus* and *EVA* software.[16] Simulated powder patterns from single-crystal determinations were generated using the *Mercury*[17] program. Experimental and calculated powder diffraction results are provided in the Supporting Information.

Results and Discussion

Synthesis. In our previous contributions, we have shown that copper(I) cyanide networks can be produced via overnight reflux reactions with KCN and bridging ligands (L).[1–3] We have since refined and simplified our strategy, determining that one hour at about 80 °C is usually sufficient to afford complete conversions to crystalline products. Thus, the preparations of a diverse group of highly luminescent materials can be effected by a simple organic solvent-free reaction carried out on a hotplate. The reactions are easily scaled up to multigram levels. The commercial low temperature polymorph of CuCN was used.[18] As indicated in Table 1, four different reactant ratios were used, leading to as few as one and as many as four different products. In those cases where multiple network products were found, increasing CuCN/L ratios led to more copper-rich products. Synthesis yields were fair to good, generally being higher for the more copper-rich products. All of the products were white, or nearly white, powders in visible light, however, and as will be described below, their luminescence responses varied widely.

Table 1. Synthetic Results for Aqueous Reflux Reactions

ligand	1:1:1[a]	2:2:1[a]	3:2:1[a]	4:2:1[a]	5:3:1[a]
Pip		**1a** (2:1)	**1a**	**1b** (20:7)	**1b**
MePip		**2** (7:2)	**2**	**2**	**2**
Me_2Pip		**3a** (2:1)	**3a**	**3b** (4:1)	**3b**
EtPip		**4** (7:2)	**4**	**4**	**4**
Et_2Pip		**5** (4:1)	**5**	**5**	**5**
BzPip		**6a** (3:2)	**6b** (5:2)	**6c** (7:2)	**6d** (4:1)
Bz_2Pip		**7** (2:1)	**7**	**7**	**7**
Ph_2CHPip		**8a** (1:1)	**8b** (2:1)	**8b**	**8b**
HMTA	**9a** (3:2)	**9b** (5:2)	**9c** (5:1)	**9c**	**9c**

[a] Mixing ratio: mmol CuCN/mmol KCN/mmol L.

The hotplate syntheses produced powders which were analytically pure and of good crystallinity (as indicated by sharp X-ray powder peaks), but sizable crystals were not present. Therefore, HT syntheses at 175 °C in Teflon-lined bombs were used to produce X-ray quality crystals. Where possible, X-ray diffraction patterns of the hotplate products were compared to calculated powder patterns from X-ray structures to confirm phase identities. As shown in Table 1, 17 distinct products were realized from bulk synthesis. Eleven of these compounds (**1b**, **2**, **3b**, **4**, **5**, **6a**, **6d**, **7**, **8b**, **9b**, and **9c**) were characterized as new X-ray structures from HT crystals and three (**1a**, **3a**, and **9a**) matched existing literature structures.[7,8] In all cases, powder-diffraction patterns from the bulk products sufficiently matched those calculated from the corresponding single crystals. This close correspondence between bulk powders and HT crystals for the diamine and tetramine ligands in the current study stands in contrast to our results with diimine L, which showed few such matches.[1]

Reactions of CuCN with Pip produced two networks, the known 2:1 product **1a** and the remarkable 20:7 product **1b**. Use of MePip or EtPip yielded networks having 7:2 ratio (**2** and **4**), irrespective of the reaction stoichiometry employed. Reactions of Me_2Pip produced the known 2:1 network **3a** and the new 4:1 **3b**. In contrast, only the 4:1 product **5** was found for Et_2Pip. The BzPip ligand gave rise to four distinct networks having 3:2 (**6a**), 5:2 (**6b**), 7:2 (**6c**), and 4:1 (**6d**) ratios. The bulkier Bz_2Pip and Ph_2CHPip were the only ligands that failed to give rise to copper-rich products having ratios >2:1. For Bz_2Pip only the 2:1 **7** was found and for Ph_2CHPip 1:1 **8a** and 2:1 **8b** formed. Finally, the tetradentate

(12) *SMART Apex II, Data Collection Software, version 2.1*; Bruker AXS Inc.: Madison, WI, 2005.
(13) *SAINT Plus, Data Reduction Software, version 7.34a*; Bruker AXS Inc.: Madison, WI, 2005.
(14) Sheldrick, G. M. *SADABS; University of Göttingen*: Göttingen, Germany, 2005.
(15) Sheldrick, G. M. *Acta Crystallogr., Sect. A* **2008**, *64*, 112.
(16) *DIFFRAC Plus, version 10.0 and EVA, release 2004*; Bruker AXS Inc.: Madison, WI, 2005.
(17) *Mercury, version 1.5*; Cambridge Crystallographic Data Centre: Cambridge, U.K., 2006.
(18) Hibble, S. J.; Eversfield, S. G.; Cowley, A. R.; Chippendale, A. M. *Angew. Chem., Int. Ed.* **2004**, *43*, 628.

HMTA yielded three networks: the known complex 3:2 complex (**9a**) and new 5:2 (**9b**) and 5:1 (**9c**) species. The previously reported synthesis of **9a** involved addition of HMTA to a hot aqueous solution of CuCN and thiosulfate or the reduction of $Cu(OAc)_2$ in the presence of water, ammonia, and formalin.[7,8] Thus, the new procedure was more convenient, albeit with equally low-product yields in the 30% range.

X-ray Structures. Eleven new X-ray structures emerged from the current study. Refinement details for all structures are summarized in Table 2 and selected bond lengths and angles are given in Table 3. A common theme in CuCN networks is the (6,3) lattice, which consists of 3-coordinate copper centers linked by cyano and L ligands to form 2D hexagonal sheets and results in $(CuCN)_2L$ stoichiometry. Lattices or sublattices with (6,3) tiling are encountered herein for networks **1b**, **2**, **3a**,[7] **4**, **5**, **6d**, and **7**. Of these, **7** is the most straightforward example because the (6,3) is the only lattice present. Interestingly, the 2:1 network **1a** does not show the (6,3) motif but rather forms a 3D network with four metal centers bridged by a single CN and associated Cu···Cu interactions.[7]

The crystal structure of **1b** has been described in a preliminary communication.[2] This compound crystallizes in the triclinic space group $P\bar{1}$. There are 20 crystallographically independent copper atoms and 20 independent cyano groups, all of which are non-symmetrically disordered. The X-ray structure of **1b** is depicted in Figure 1. Two nonidentical sublattices are present. Sublattice A (containing copper atoms Cu9−Cu20) is a (6,3) lattice lying in the *a*,*b* plane and consisting of hexagonal $Cu_6(CN)_4(Pip)_2$ units. There are three independent, but essentially identical, A sublattices (Cu9/Cu10/Cu15/Cu16, Cu11/Cu14/Cu17/Cu20, and Cu12/Cu13/Cu18/Cu19). The three A layers stack in an XYZZYX... pattern. Despite the 3-coordination of the copper atoms, the cyano−Cu−cyano angles are relatively obtuse, measuring 141.58(19)−143.6(2)°. These large angles suggest a predominance of CuCN chain bonding over Pip coordination. For **1b** and most of the other (6,3) sublattices, metal-atom attachment to the piperazines is axial. As a result, the ligand is oriented perpendicular to the A sheet plane and creates a series of zigzag steps in the sheets.

Sublattice B (containing Cu1−Cu8) consists mostly of roughly linear 2-coordinate copper atoms, forming CuCN chains, which are cross-linked at every eighth copper by a Pip unit. This arrangement in the B sublattice produces rippled sheets of large tiled $Cu_{18}(CN)_{16}(Pip)_2$ rings, which are threaded through the hexagonal voids in the A sublattices. Sublattices A and B have stoichiometries $(CuCN)_2(Pip)$ and $(CuCN)_8(Pip)$, respectively. The 6:1 A/B ratio gives rise to a $6[(CuCN)_2(Pip)]\cdot[(CuCN)_8(Pip)]$ formulation, or more simply, $(CuCN)_{20}(Pip)_7$. The Pip centroids in the two sublattices lie roughly in line with one another, but the rings are rotated by about 90° with respect to one another and are canted at different angles as well. Interestingly, although copper is coordinated in axial positions to Pip in the A sublattice, it is in equatorial position in the B sublattice. There are a total of 10 Cu···Cu interactions that are close to the 2.8 Å van der Waals distance (Cu···Cu = 2.8156(10)−3.0378(11) Å). All of these weak interactions are between the two subnetworks and are unsupported by any ligand bridging.

The MePip and EtPip **2** and **4** are isomorphic and isostructural to one another (Figure 2). Each has the formula $(CuCN)_7L_2$ and crystallizes in the monoclinic *C*2/*m* space group. Each shows seven independent copper atoms, all of which lie on a single mirror plane. All cyanides are disordered; X1/X1 and X2/X2 are symmetrically disordered (X = disordered C/N). As was the case with **1b**, two sublattice types are present. In direct analogy to **1b**, sublattice A contains 3-coordinate metal atoms and forms a (6,3) $(CuCN)_2L$ stepped sheet running in the *a*,*b* plane. There are two independent A sublattices (Cu4/Cu5 and Cu6/Cu7), which are related by 2-fold rotation and stack in XYYX... sequence. Cyano−Cu−cyano angles for the 3-coordinate *A* centers are again large: 141.59(13)−145.85(14)° in **2** and 141.42(18)−145.77(17)° in **4**. The *B* sublattices in **2** and **4** are simple CuCN chains, lacking any L cross-links. The chains, which propagate parallel to the *c* axis and thread through the (6,3) sheets, undulate, owing to the <180° cyano−Cu−cyano bond angles: 152.71(15)−172.05(13)° in **2** and 146.3(2)−171.21(17)° in **4**. As is the case for **1b**, the sublattices are weakly linked by near-van der Waals interactions of 2.6087(7), 2.7369(7) and 2.8824(7) Å in **2** and 2.7076(11), 2.7824(9), and 2.9639(10) Å in **4**. The A and B sublattices occur in 3:2 ratio: $2[(CuCN)_2L]\cdot 3CuCN$. Copper atoms are coordinated in axial positions to the piperazine chairs in both **2** and **4**.

A straightforward (6,3) network is recognized for $(CuCN)_2(Me_2Pip)$ (**3a**),[7] but no such formulation appears to exist for L = Et_2Pip. The $(CuCN)_4L$ **3b** and **5** are similar but are not isostructural (see Figures 3 and 4). Complex **3b** crystallizes in the orthorhombic *Cccm* space group and **5** crystallizes in *C*2/*m*. Both structures are composed of two half-independent copper atoms and one-half- and two-quarter-independent cyano groups, all of which are symmetrically disordered. In these structures a single (6,3) A stepped sheet sublattice (Cu1) is penetrated by a CuCN chain B sublattice (Cu2). Although all of the B chains in **5** propagate in a parallel direction, alternate B chains in **3b** run in orthogonal directions. However, in both **3b** and **5** (as with **2** and **4**) all CuCN chains run through the hexagonal voids in the A sublattice. In these networks, the sublattice ratio is $[(CuCN)_2L]\cdot 2CuCN$. Copper atoms are coordinated in axial positions to the piperazine chairs in both **3b** and **5**. The cyano-Cu-cyano angles in **3b** and **5** are 142.99(10) and 143.97(13)° for Cu1 and 148.28(13) and 158.37(11)° for Cu2. Near-van der Waals Cu···Cu interactions between the sublattices measuring 2.5893(7) and 2.6715(6) Å in **3b** and **5**, respectively, are present.

Network **6a**, $(CuCN)_3(BzPip)_2$, crystallizes in the chiral monoclinic space group $P2_1$. Six independent copper atoms and six cyano groups are present. Five of the latter are non-symmetrically disordered and one (C2/N2) is fully ordered. The resulting network is composed of planar rows of undulating CuCN chains running roughly parallel to the *a* axis (Figure 5). The chains are cross-linked by bridging L

Table 2. Crystal and Structure Refinement Data

	1b	2	3b
CCDC deposit no.	647 769	678 228	678 225
color and habit	colorless prism	colorless blade	colorless prism
size, mm^3	0.19 × 0.13 × 0.06	0.42 × 0.23 × 0.05	0.26 × 0.13 × 0.05
formula	$C_{48}H_{70}Cu_{20}N_{34}$	$C_{17}H_{24}Cu_7N_{11}$	$C_5H_7Cu_2N_3$
fw	2394.18	827.25	236.22
space group	$P\bar{1}$ (No. 2)	*C*2/*m* (No. 12)	*Cccm* (No. 66)
a, Å	8.4553(2)	13.9138(2)	12.10260(10)
b, Å	15.7200(3)	9.41970(10)	14.16340(10)
c, Å	27.6308(6)	21.1231(3)	9.37560(10)
α, deg	91.9900(10)	90	90
β, deg	93.9660(10)	105.9470(10)	90
γ, deg	97.2830(10)	90	90
V, $Å^3$	3530.75(14)	2661.93(6)	1607.11(2)
Z	2	4	8
ρ_{calcd}, g cm^{-3}	2.190	2.064	1.953
F_{000}	2352	1624	928
μ(Cu Kα), mm^{-1}	6.591	6.272	5.930
radiation (*λ*, Å)	Cu Kα (1.54178)	Cu Kα (1.54178)	Cu Kα (1.54178)
T, K	296	100	100
residuals:[a] R; R_w	0.0506; 0.1529	0.0255; 0.0672	0.0229; 0.0541
GOF	1.054	1.149	1.081

	4	5	6a
CCDC deposit no.	678 229	678 230	678 234
color and habit	colorless blade	colorless blade	colorless plate
size, mm^3	0.25 × 0.09 × 0.03	0.31 × 0.05 × 0.02	0.30 × 0.23 × 0.02
formula	$C_{19}H_{28}Cu_7N_{11}$	$C_6H_9Cu_2N_3$	$C_{50}H_{64}Cu_6N_{14}$
fw	855.30	250.24	1242.39
space group	C2/*m* (No. 12)	*C*2/*m* (No. 12)	$P2_1$ (No. 4)
a, Å	13.8422(2)	13.1088(3)	19.3691(4)
b, Å	9.41320(10)	9.3972(2)	6.82790(10)
c, Å	21.6258(2)	9.5547(4)	21.6030(4)
α, deg	90	90	90
β, deg	101.9110(10)	133.1290(10)	108.0350(10)
γ, deg	90	90	90
V, $Å^3$	2757.16(6)	859.00(4)	2716.63(9)
Z	4	4	2
ρ_{calcd}, g cm^{-3}	2.060	1.935	1.519
F_{000}	1688	496	1272
μ(Cu Kα), mm^{-1}	6.082	5.590	5.995
radiation (*λ*, Å)	Cu Kα (1.54178)	Cu Kα (1.54178)	Cu Kα (1.54178)
T, K	296	296	200
residuals:[a] R; R_w	0.0298; 0.0716	0.0216; 0.0570	0.0273; 0.0692
GOF	1.080	1.043	0.994

	6d	7	8b
CCDC deposit no.	678 233	678 231	678 232
color and habit	colorless blade	colorless plate	colorless prism
size, mm^3	0.24 × 0.11 × 0.02	0.17 × 0.13 × 0.04	0.31 × 0.14 × 0.06
formula	$C_{15}H_{16}Cu_4N_6$	$C_{10}H_{11}Cu_1N_2$	$C_{19}H_{21}Cu_2N_4$
fw	534.50	222.75	432.48
space group	*Pnma* (No. 62)	$P2_1/c$ (No. 14)	*Pbca* (No. 61)
a, Å	18.8238(5)	9.37890(10)	11.58880(10)
b, Å	9.2760(2)	13.1246(2)	8.73360(10)
c, Å	10.9423(3)	9.49180(10)	35.7412(3)
α, deg	90	90	90
β, deg	90	118.1060(10)	90
γ, deg	90	90	90
V, $Å^3$	1910.63(8)	1030.61(2)	3617.44(6)
Z	4	4	8
ρ_{calcd}, g cm^{-3}	1.858	1.436	1.588
F_{000}	1056	456	1768
μ(Cu Kα), mm^{-1}	5.995	2.609	1.588
radiation (*λ*, Å)	Cu Kα (1.54178)	Cu Kα (1.54178)	Cu Kα (1.54178)
T, K	100	296	100
residuals:[a] R; R_w	0.0201; 0.0523	0.0262; 0.0731	0.0265; 0.0717
GOF	1.068	1.068	1.038 m

	9b	9c
CCDC deposit no.	678 226	678 227
color and habit	colorless block	colorless needle
size, mm^3	0.16 × 0.15 × 0.10	0.15 × 0.03 × 0.02

Table 2. Continued

	9b	9c
formula	$C_{34}H_{48}Cu_{10}N_{26}$	$C_{44}H_{48}Cu_{20}N_{36}$
fw	1456.38	2351.98
space group	*C*2/*c* (No. 15)	$P2_1/c$ (No. 14)
a, Å	21.7147(9)	7.0745(2)
b, Å	6.9228(3)	29.9449(7)
c, Å	15.6273(7)	14.7420(3)
α, deg	90	90
β, deg	111.294(2)	92.7030(10)
γ, deg	90	90
V, Å^3	2188.82(16)	3119.55(13)
Z	2	2
ρ_{calcd}, g cm^{-3}	2.210	2.504
F_{000}	1448	2288
μ(Cu Kα), mm^{-1}	5.691	7.669
radiation (λ, Å)	Cu Kα (1.54178)	Cu Kα (1.54178)
T, K	173	173
residuals:[a] R; R_w	0.0250; 0.0636	0.0331; 0.0747
GOF	1.107	1.029

[a] $R = R_1 = \sum||F_o| - |F_c||/\sum|F_o|$ for observed data only. $R_w = wR_2 = \{\sum[w(F_o^2 - F_c^2)^2]/\sum[w(F_o^2)^2]\}^{1/2}$ for all data.

in the *c* direction, forming 2D double sheets, which are capped by nonbridging L. All copper atoms are 3-coordinate, having cyano−Cu−cyano bond angles of 128.53(12)−140.28(12)°. Each metal atom coordinates two cyanides and a single BzPip. The four BzPip ligands in the structure show interesting contrasts. Two are bridging, connecting Cu1 & Cu2 and Cu4 & Cu5, linking pairs of CuCN chains. These BzPip groups bond copper in equatorial positions at the H-substituted end and in axial positions at the benzyl-substituted end. The remaining two BzPip ligands are terminal. These BzPip ligands bond Cu3 and Cu6 at the H-substituted end in axial positions. The benzyl-substituted ends are not coordinated. Among the six Cu−N(BzPip) bonds, the two Cu−NBz bonds are longer than the Cu−NH bonds, by 0.02-0.05 Å. Two Cu···Cu interactions are present: Cu3···Cu4 = 2.6650(6) and C1···Cu6 = 2.9644(6) Å. Cyanide X4/X4, which bridges Cu4 and Cu5, shows a weak bridging interaction to Cu3. This is indicated by the slight bending of Cu4−X4−X4 angle (156.1(3)°) toward Cu3.

As shown in Figure 6, **6d** (which crystallizes in the orthorhombic group *Pnma*) is structurally related to the other $(CuCN)_4L$ **3b** and **5**. A highly rippled (6,3) sheet (sublattice A) is created by 3-coordinate atoms Cu3 and Cu4. Sublattice B CuCN chains are formed by Cu1 and Cu2, running parallel to the *a* axis and passing through the A sheets. The cyano−Cu−cyano angles are 157.84(10) and 162.49(10)° for 2-coordinate centers and 138.59(10) and 140.67(10)° for the 3-coordinate centers. All four copper atoms are half-independent. Two of three cyano groups are also centered about special positions; all three cyano groups are non-symmetrically disordered. The half-independent BzPip coordinates copper equatorially on the NH side and axially on the benzyl end; the Cu−NBz bond is ca. 0.04 Å longer than the Cu−NH. As with **3b** and **5**, metal−metal interactions (2.6171(5) and 2.6387(5) Å) are present, linking the two sublattices.

The structure of **7**, in space group $P2_1/c$, is that of a simple (6,3) sheet running parallel to the *b*,*c* plane (Figure 7). In other words, **7** consists of an A sublattice only. A single 3-coordinate copper atom is bridged by a non-symmetrically disordered cyanide and a half-independent Bz_2Pip unit. Both metal atom attachments to the disubstituted piperazine are axial, resulting in a series of zigzag steps in the sheet. The Cu−NBz value of 2.2149(14) is the longest Cu−N(L) distance in the current study. The cyano−Cu−cyano angle is 147.82(8)°. Predictably, there are no Cu···Cu interactions. Of the (6,3) networks in this study, only **7** does not appear to allow penetration by a second sublattice. For all of the smaller piperazines studied (Pip, MePip, Me_2Pip, EtPip, Et_2Pip, and BzPip), threading of CuCN through the honeycomb (6,3) lattice results in copper-rich (i.e., >2:1) phases. The likely explanation is that benzyl groups in **7** block access to the channels.

The very bulky substitution on one end of Ph_2CHPip precludes metal coordination, leading to the unique structure of **8b**, which is shown in Figure 8. The space group is orthorhombic *Pbca*. A zigzag chain running parallel to the *b* axis is formed by 3-coordinate Cu1 and cyano X1/X1. Connected to Cu1 and decorating the chain along the *a* axis are X2−X2−Cu2−L units. Because the metal is coordinated axially to the terminal Ph_2CHPip units, the ligands are oriented away from the plane of the chain, in roughly the *c* direction. Ligand-free sides of adjacent CuCN chains face one another, with the nearest approach of Cu1···Cu2 = 2.8976(4) Å. Both copper atoms show coordination environments that are unique in the current study. Three-coordinate Cu1 lies in $Cu(CN)_3$ coordination. The angles around Cu1 deviate by <5° from 120°. The $Cu(CN)_3$ coordination sphere is very unusual in CuCN−L networks, having been seen previously only for the $(CuCN)_3$(2,4-diaminopyrimidine) and $(CuCN)_5(pyridazine)_2$.[1] Two-coordinate Cu2 is in cyano-Cu-L coordination and shows a 163.78(7)° bond angle. In previously characterized monodentate amine complexes of CuCN, decoration of the chains consists merely of pendant amine ligands (L), rather than cyano−Cu−L side chains.[7,19,20] The only precedent for this 2-coordinate arrangement is the cyano−Cu−OH_2 unit seen in $(CuCN)_3(H_2O)$.[21]

Two new CuCN−HMTA networks (**9b** and **9c**) were elucidated during the current study. The literature structure

(19) Dyason, J. C.; Healy, P. C.; Engelhardt, L. M.; Pakawatchai, C.; Patrick, V. A.; White, A. H. *J. Chem. Soc., Dalton Trans.* **1985**, 839.
(20) Bowmaker, G. A.; Lim, K. C.; Skelton, B. W.; White, A. H. *Z. Naturforsch.* **2004**, *59b*, 1264.
(21) Kildea, J. D.; Skelton, B. W.; White, A. H. *Aust. J. Chem.* **1985**, *38*, 1329.

Table 3. Selected Bond Lengths and Angles for All Complexes[a]

		1b, $(CuCN)_{20}(Pip)_7$	
Cu−X	1.843(5)−1.900(4)	Cu−X−X	160.9(6)−178.8(4)
X−X	1.128(8)−1.168(6)	X−Cu[b]−X	134.5(3)−143.6(2)
Cu−N	2.049(7)−2.144(4)	X−Cu[c]−X	165.2(3)−179.76(19)
Cu−Cu	2.8156(10)−3.0378(11)	X−Cu−N	103.7(2)−114.8(2)
		2, $(CuCN)_7(MePip)_2$	
Cu−X	1.851(3)−1.896(2)	Cu−X−X	172.2(3)−179.9(3)
X−X	1.149(7)−1.169(7)	X−Cu[b]−X	141.59(13)−145.85(14)
Cu−N	2.081(3)−2.143(3)	X−Cu[c]−X	152.71(15)−172.05(13)
Cu−Cu	2.6087(7)−2.8824(7)	X−Cu−N	106.70(7)−109.16(7)
		3b, $(CuCN)_4(Me_2Pip)$	
Cu−X	1.860(3)−1.884(2)	Cu−X−X	173.8(4)−177.0(2)
X−X	1.147(4)−1.149(6)	X1−Cu1[b]−X1	143.99(13)
Cu1−N4	2.112(2)	X2−Cu2[c]−X3	148.28(13)
Cu1−Cu2	2.5893(7)	X1−Cu1−N4	107.74(7)
		4, $(CuCN)_7(EtPip)_2$	
Cu−X	1.858(4)−1.900(3)	Cu−X−X	169.9(4)−179.6(4)
X−X	1.144(4)−1.153(5)	X−Cu[b]−X	141.21(16)−145.77(17)
Cu−N	2.100(3)−2.158(3)	X−Cu[c]−X	146.3(2)−171.21(17)
Cu−Cu	2.6539(9)−2.9639(10)	X−Cu-N	106.43(8)−109.38(8)
		5, $(CuCN)_4(Et_2Pip)$	
Cu−X	1.863(3)−1.8927(16)	Cu−X−X	176.0(2)−179.2(3)
X−X	1.141(5)−1.149(3)	X2−Cu2[c]−X3	158.37(12)
Cu1−N4	2.137(2)	X1−Cu1−N4	108.50(5)
Cu1−Cu2	2.6715(6)	X1−Cu1[b]−X1′	142.99(10)
		6a, $(CuCN)_3(BzPip)_2$	
Cu−X	1.872(3)−1.953(3)	Cu−X−X	156.1(3)−176.5(3)
X−X	1.144(4)−1.160(4)	X−Cu[b]−X	128.53(12)−140.28(12)
Cu−N	2.100(2)−2.124(2)	X−Cu−N	100.09(15)−124.97(14)
Cu−Cu	2.6650(6), 2.9644(6)		
		6d, $(CuCN)_4(BzPip)$	
Cu−X	1.852(2)−1.8966(17)	Cu−X−X	172.8(2)−179.8(2)
X−X	1.162(3)−1.165(3)	X−Cu[b]−X	138.59(10), 140.67(10)
Cu−N	2.141(2), 2.100(2)	X−Cu[c]−X	157.84(10), 162.49(10)
Cu−Cu	2.6171(5), 2.6387(5)	X−Cu−N	109.64(5), 110.16(5)
		7, $(CuCN)_2(Bz_2Pip)$	
Cu1−X1	1.873(2), 1.9024(17)	Cu1−X1−X1′	175.66(17), 176.25(18)
X1−X1′	1.144(3)	X1−Cu1[b]−X1	147.82(8)
Cu1−N2	2.2149(14)	X1−Cu1−N2	98.63(6), 113.53(7)
		8b, $(CuCN)_2(Ph_2CHPip)$	
Cu1−X1	1.8963(19)−1.9417(18)	Cu−X−X	169.96(16)−176.50(16)
X−X	1.157(3), 1.162(3)	X1−Cu1[b]−X2	114.65(7)−124.43(8)
Cu2−N3	1.9349(15)	X2−Cu2[c]−N3	163.78(7)
Cu1−Cu2	2.8976(4)		
		9b, $(CuCN)_5(HMTA)_2$	
Cu−X	1.926(2)−1.940(2)	Cu−X−X	164.77(19)−173.1(3)
Cu−X[d]	1.993(2)−2.380(2)	Cu−X[d]−X	119.68(18)−165.4(2)
X−X	1.156(3)−1.163(5)	X−Cu−X	103.90(8)−121.48(9)
Cu−N	2.1664(19)−2.1913(18)	Cu−X[d]−Cu	74.61(7), 71.20(8)
Cu−Cu	2.4381(6), 2.6682(7)	X−Cu−N	92.34(7)−127.04(8)
		N−Cu−N	107.03(10)
		9c, $(CuCN)_5(HMTA)$	
Cu−X	1.830(4)−2.028(4)	Cu−X−X	166.7(4)−178.8(4)
Cu−X[d]	1.920(5)−2.444(4)	Cu−X[d]−X	109.4(3)−176.9(4)
X−X	1.147(6)−1.167(6)	X−Cu[b]−X	94.44(14)−127.50(16)
Cu−N	2.103(4)−2.217(4)	X−Cu[c]−X	166.66(17), 168.67(17)
Cu−Cu	2.4098(12)−2.5577(13)	Cu−X[d]−Cu	68.39(13)−75.22(15)
		X−Cu−N	92.90(14)−123.21(15)

[a] X indicates cyanide C/N, N indicates L ligand. [b] 3-Coordinate copper atom. [c] 2-Coordinate copper atom. [d] X atom bridges two copper atoms.

of **9a** reveals only a slight alteration to the familiar (6,3) motif, with all HMTA ligands bidentate and alternating 3- and 4-coordinate copper atoms.[8] The resulting sheets are tiled from alternating $Cu_4(CN)_2(HMTA)_2$ and $Cu_6(CN)_4(HMTA)_2$ rings. In contrast, **9b** and **9c** (Figures 9 and 10) contain 3- and 4-coordinate HMTA units, respectively, and are far more structurally complex 3D materials. There is also a distinct tendency toward cyano-bridged dimer formation. This is probably the result of the forced close proximity of copper centers in **9b** and **9c**.

In **9b** (monoclinic *C*2/*c*), each of the two fully independent copper atoms (Cu1 and Cu2) forms part of a cyano-bridged $Cu_2(CN)_2$ dimer with short Cu···Cu interactions (2.4381(6), 2.6682(7) Å). Each dimer links to four cyanides (including the two that bridge the metal atoms) and two HMTA units. The half-independent Cu3 is 4-coordinate, binding two

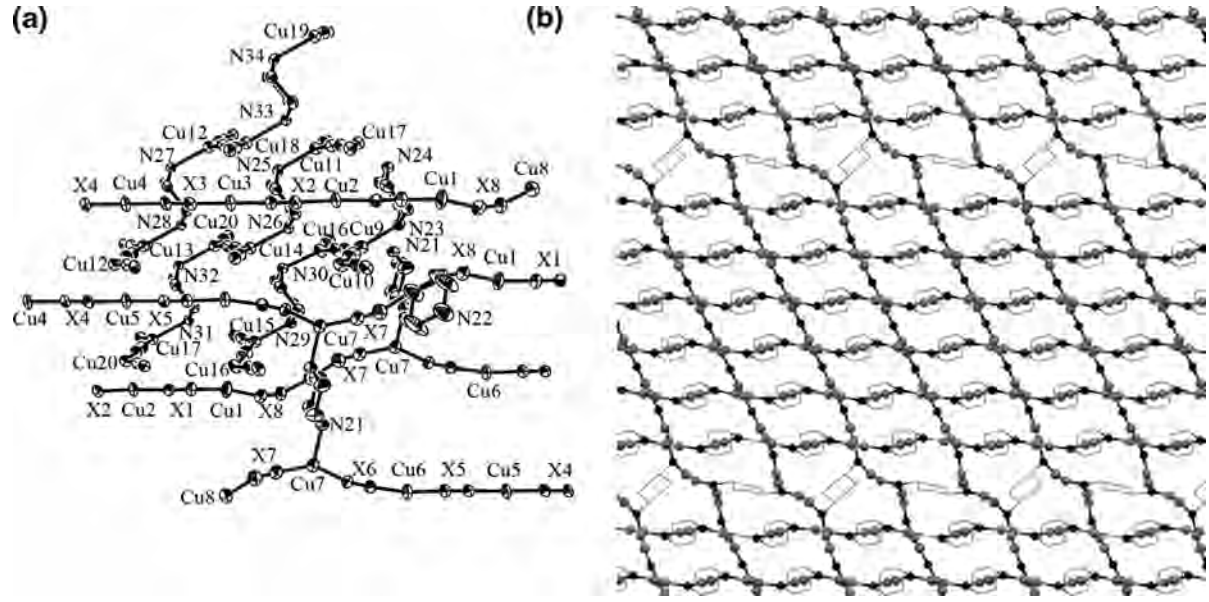

Figure 1. X-ray crystal structure of $(CuCN)_{20}(Pip)_7$, **1b**. Hydrogen atoms and Cu···Cu interactions omitted for clarity. (a) Thermal ellipsoid view (50%). (b) Projection down crystallographic *a* axis. Atom identities for all ball and stick projections: black circles = Cu atoms; gray circles = cyano C/N atoms; wireframe = L ligand.

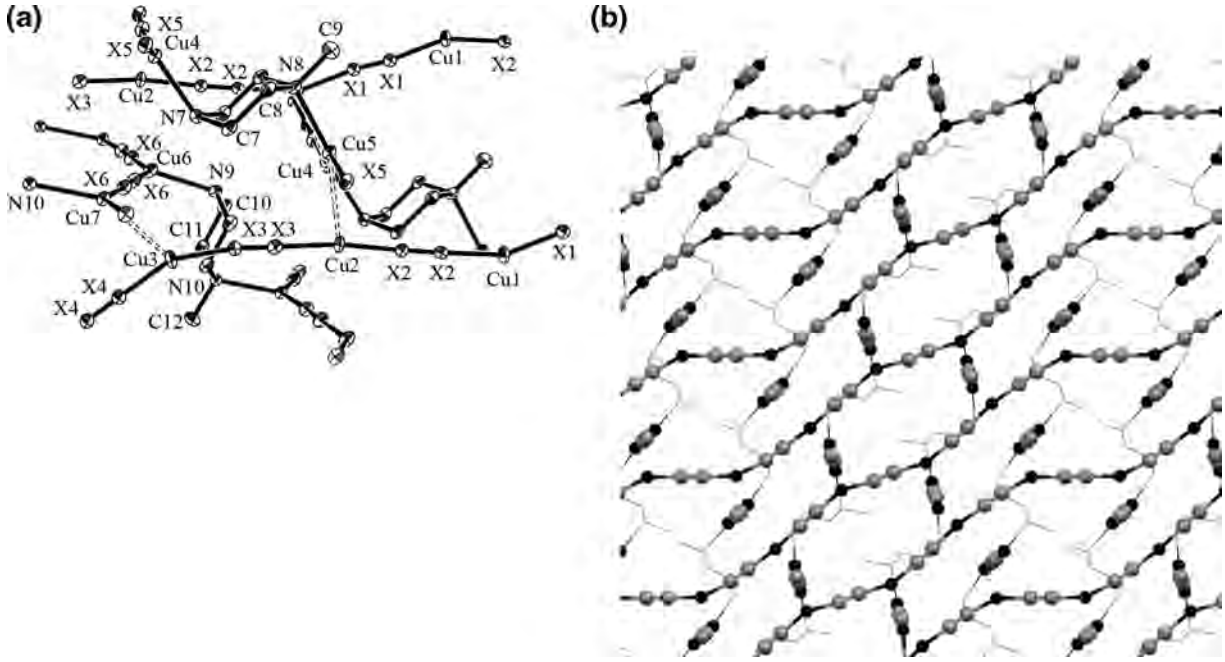

Figure 2. X-ray crystal structure of $(CuCN)_7(MePip)_2$, **2**. Hydrogen atoms omitted for clarity (a) Thermal ellipsoid view (50%). All Cu···Cu interactions are shown with dashed bonds. (b) Projection down crystallographic *b*-axis. Cu···Cu interactions are not shown.

cyanides and two HMTA units. Copper atoms are coordinated to three of the four HMTA nitrogen atoms. The 3D structure of **9c** ($P2_1/c$) reveals 10 fully independent copper atoms and 2 independent HMTA units, both of which coordinate copper at all four nitrogen atoms. Four $Cu_2(CN)_2$ dimers like those in **9b** are present; each shows a short Cu···Cu interaction (2.4098(12)−2.5577(13) Å). However, unlike **9b** two 2-coordinate copper atoms (Cu7 and Cu10) are also present. Each is coordinated in nearly linear fashion to two cyanides. These atoms are reminiscent of the 2-coordinate metal centers in **1b**, **2**, **3b**, **4**, **5**, and **6d**; however, in the present case they are part of the main network, rather than independent CuCN chains. These 2-coordinate centers appear to help create some extra space in this very dense (ca. 2.50 g/cm^3) network. The potentially tetradentate HMTA ligand has now been shown to form bi-, tri-, and tetradentate coordination in CuCN networks. **9c** represents one of relatively few occurrences of tetradentate HMTA in network materials; most of the recognized examples are based on Ag(I).[22]

Survey of CuCN−L Networks. There are now some 55 known CuCN−L (L = bridging bidentate diamine or diimine ligand) networks, 32 of which are associated with this or our previous study.[1–3,6–8] The products break down by stoichiometry as follows: 6 (CuCN)L, 4 $(CuCN)_3L_2$, 21 $(CuCN)_2L$, 4 $(CuCN)_5L_2$, 8 $(CuCN)_3L$ (including the 20:7

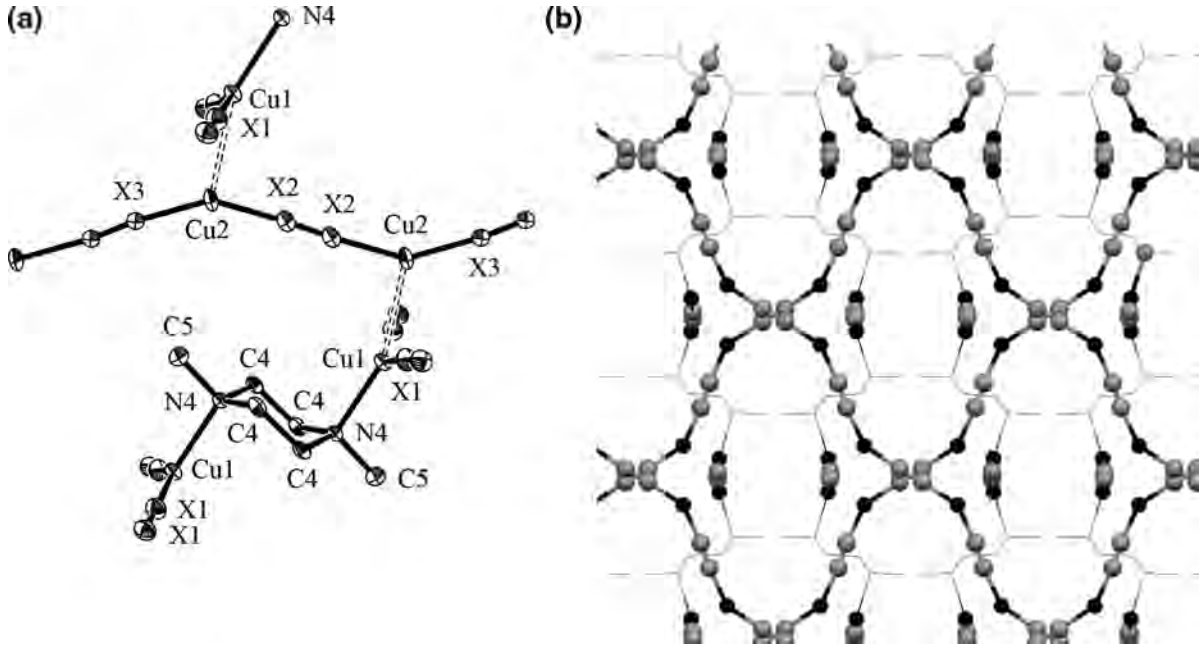

Figure 3. X-ray crystal structure of $(CuCN)_4(Me_2Pip)$, **3b**. Hydrogen atoms omitted for clarity (a) Thermal ellipsoid view (50%). All Cu···Cu interactions are shown with dashed bonds. (b) Projection down crystallographic *c* axis. Cu···Cu interactions are not shown.

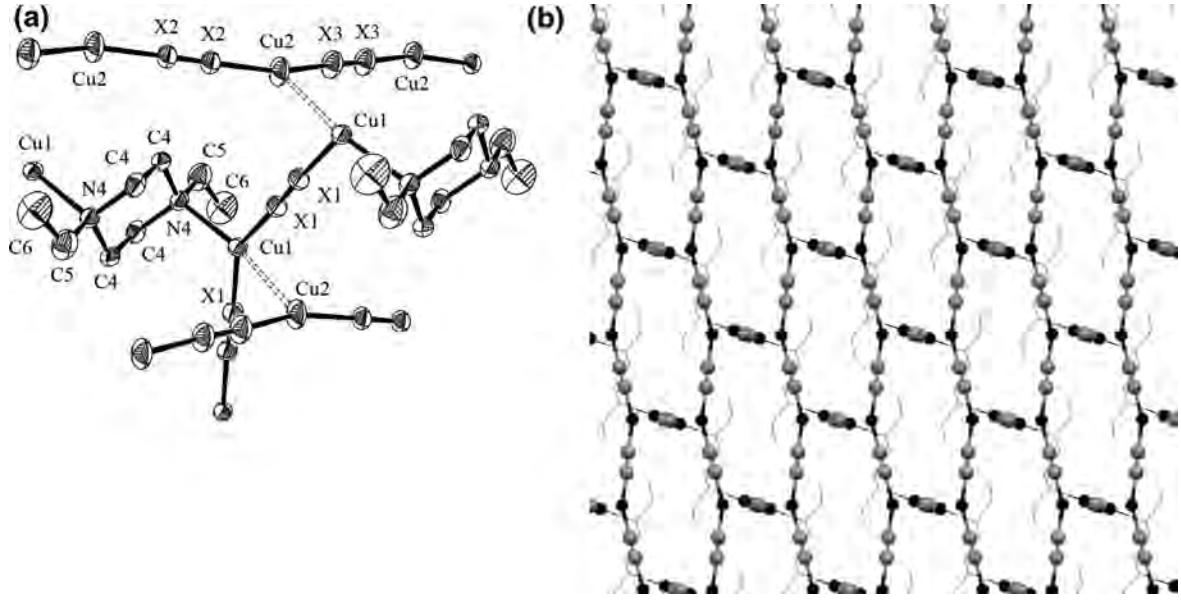

Figure 4. X-ray crystal structure of $(CuCN)_4(Et_2Pip)$, **5**. Hydrogen atoms omitted for clarity. (a) Thermal ellipsoid view (50%). All Cu···Cu interactions are shown with dashed bonds. (b) Projection down crystallographic *b* axis. Cu···Cu interactions are not shown.

product **1b**), 6 $(CuCN)_7L_2$, and 6 $(CuCN)_4L$. All 1:1 CuCN−L compounds exhibit 4-coordinate copper. The 3:2 compounds display either 2- and 4- or 3- and 4-coordination. The 2:1 networks all show only 3-coordinate copper. Finally, the 5:2, 3:1, 7:2, and 4:1 species have both 2- and 3-coordination. It will be noted that even number ratios are more common than odd ratios by more than two-to-one margin, suggesting a preference for the relative structural simplicity associated with these ratios.

The most common network type is $(CuCN)_2L$. This fact suggests a preference for 3-coordinate copper. One common arrangement for such complexes is the (6,3) network, consisting of cross-linked CuCN chains forming tiled $Cu_6(CN)_4L_2$ rings. Such is the case for **3a**[7] and **7** in the current study, and also for L = 2-aminopyrimidine, quinoxaline, and phenazine.[1,6f] Copper−copper bridging is sometimes found in 2:1 complexes, producing a 3D honeycomb arrangement, as occurs for **1a** (Cu···Cu = 2.581(1) Å)[7] and for several other 2:1 compounds.[1] However, in the present case, the simple (6,3) sheet arrangement is of greater interest, because it lies at the heart of many of the most luminescent networks (see below). The **3a** and **7** networks are very similar, having obtuse cyanide−Cu−cyanide angles and large hexagonal channels.

The hexagonal channels in the (6,3) networks allow for penetration by a second sublattice, which usually takes the form of CuCN chains. This is not so for **7**, in which benzyl groups block access to the channels. Nevertheless, for L =

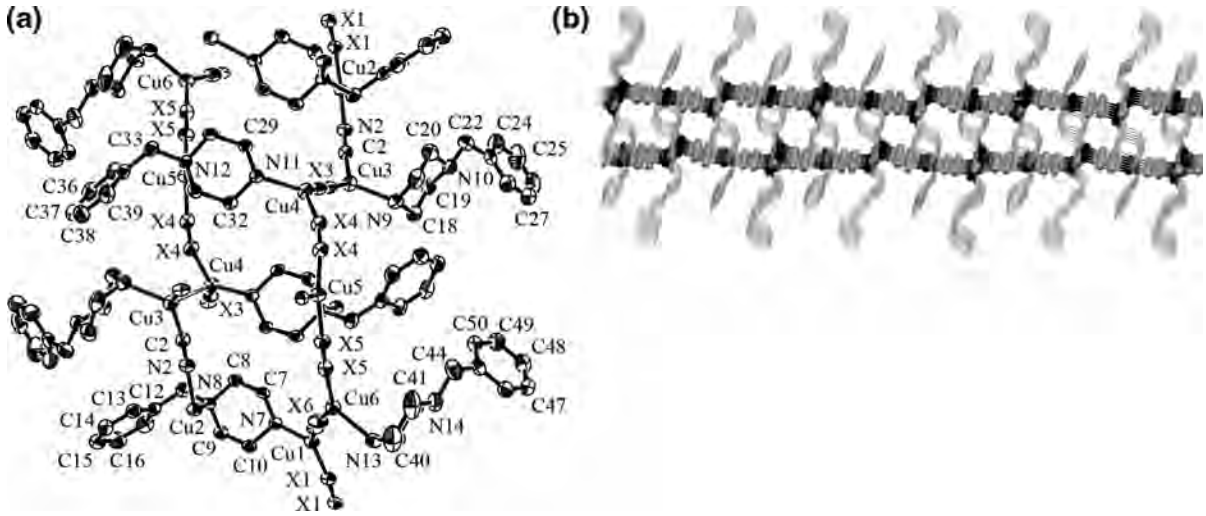

Figure 5. X-ray crystal structure of $(CuCN)_3(BzPip)_2$, **6a**. Hydrogen atoms omitted for clarity. (a) Thermal ellipsoid view (50%). All Cu···Cu interactions are shown with dashed bonds. (b) Projection down crystallographic *b* axis. Cu···Cu interactions are not shown.

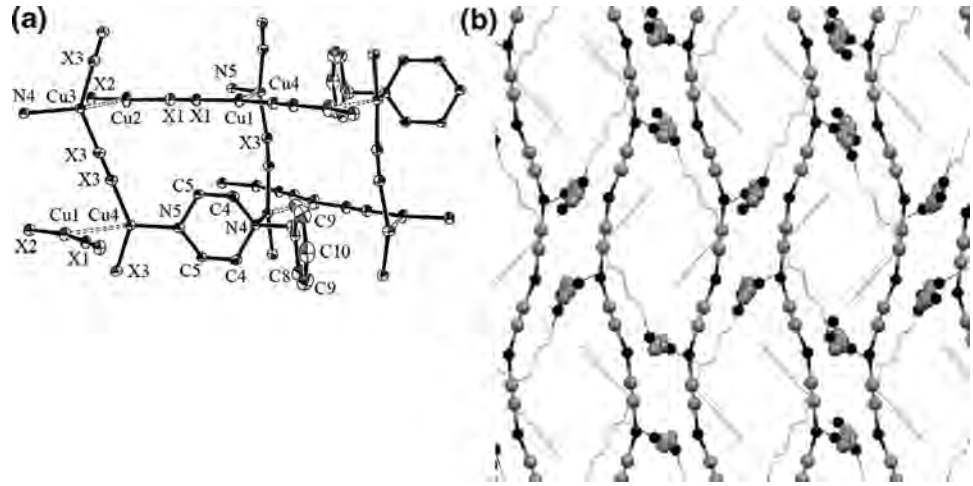

Figure 6. X-ray crystal structure of $(CuCN)_4(BzPip)$, **6d**. Hydrogen atoms omitted for clarity. (a) Thermal ellipsoid view (50%). All Cu···Cu interactions are shown with dashed bonds. (b) Projection down crystallographic *b* axis.

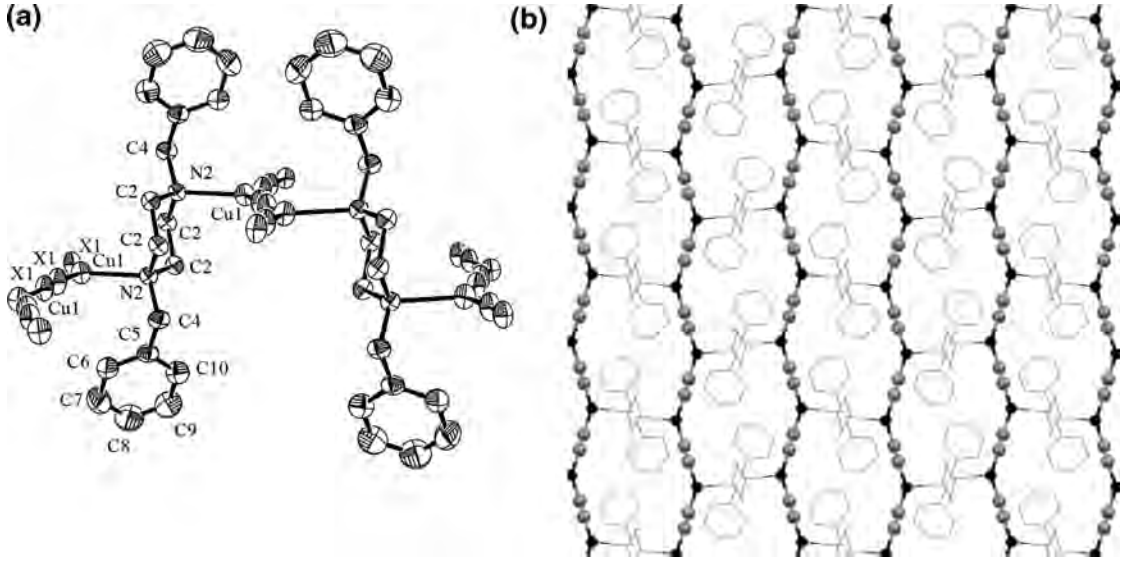

Figure 7. X-ray crystal structure of $(CuCN)_2(Bz_2Pip)$, **7**. Hydrogen atoms omitted for clarity. (a) Thermal ellipsoid view (50%). (b) Projection down crystallographic *a* axis.

Pip, MePip, Me_2Pip, EtPip, Et_2Pip, and BzPip, Cu-rich (i.e., >2:1) phases have been found. All of these products (**1b**, **2**, **3b**, **4**, **5**, and **6d**) have CuCN threading and all but **6d** are luminescent. The CuCN chains run roughly perpendicular

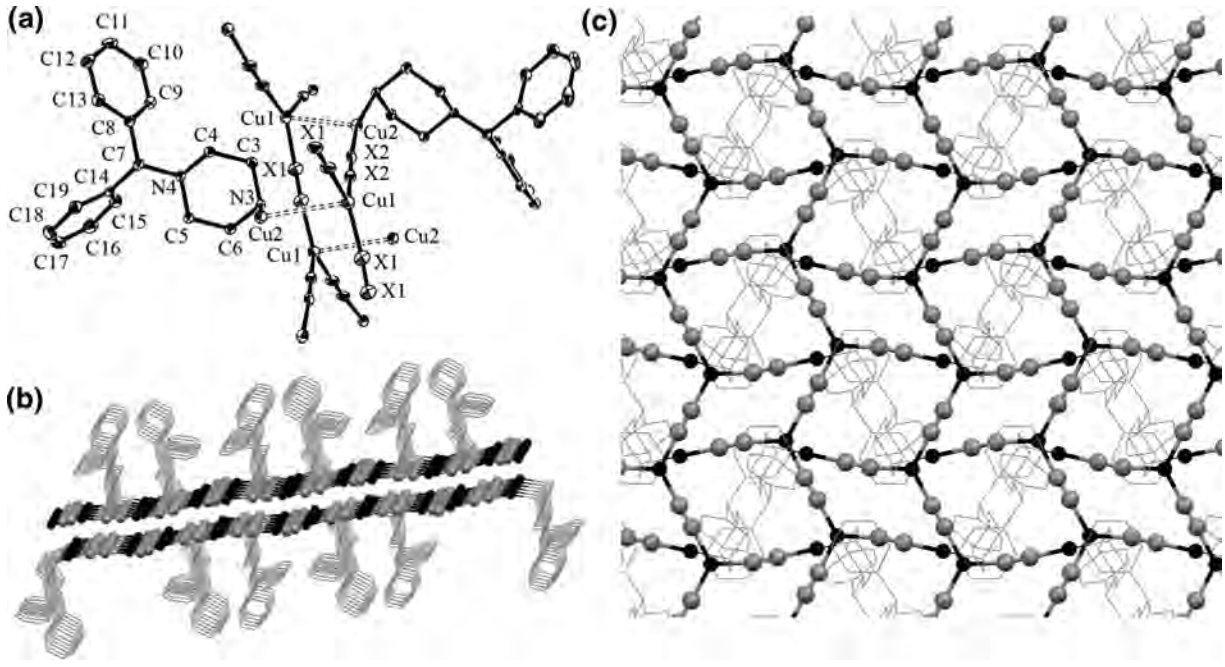

Figure 8. X-ray crystal structure of $(CuCN)_2(Ph_2CHPip)$, **8b**. Hydrogen atoms omitted for clarity. (a) Thermal ellipsoid view (50%). (b) Projection down the crystallographic *c* axis. Cu···Cu interactions are not shown. (c) Projection down crystallographic *b* axis. Cu···Cu interactions are not shown.

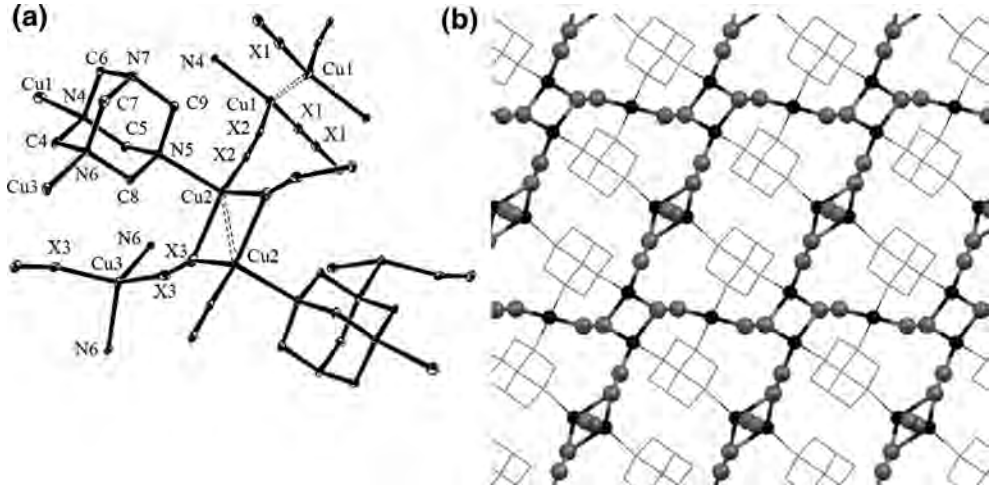

Figure 9. X-ray crystal structure of $(CuCN)_5(HMTA)_2$, **9b**. Hydrogen atoms omitted for clarity. (a) Thermal ellipsoid view (50%). All Cu···Cu interactions are shown with dashed bonds. (b) Projection down crystallographic *b* axis. Cu···Cu interactions are not shown.

to the (6,3) sheets, passing through the channels, which are roughly 10 × 8 Å in all cases. Similar behavior has been found for $(CuCN)_3$(pyrazine) and $(CuCN)_n$(4,4′-bipyridine) (n = 3.5, 4).[6e,f,i] In several cases, including $(CuCN)_7$(pyrimidine)$_2$, $(CuCN)_4$(quinazoline), $(CuCN)_7$(phthalazine)$_2$, both 2- and 3-coordinate copper centers are actually incorporated into a single L-cross-linked lattice.[1] The unusual $(CuCN)_4$(1,4-bis(imidazole-1-ylmethyl)benzene) contains 2-coordinate copper atoms both within the cross-linked sublattice and as independent chains.[6k] Uniquely, in **1b** the CuCN chains coordinate a Pip ligand at every eighth copper center, producing a sublattice of long interlocking $Cu_{18}(CN)_{16}(Pip)_2$ rings.[2] In all of these compounds, the 3-coordinate cyanide−Cu−cyanide angles are very open (134.5(3)−157.1(3)°), suggesting significant 2-coordinate (CuCN) character. In contrast, it will be noted that the 3-coordinate $Cu(CN)_3$ angles in **8b** are very close to 120°.

Thermal Analysis. As in our previous study, thermogravimetric analysis (TGA) of CuCN−L networks yielded smooth loss of L, thus providing sufficiently reliable data for rapid determination of product stoichiometry.[1] Mass losses, temperature ranges, and interpretations for the bulk powders in the current study provided in the Experimental

(22) (a) Bertelli, M.; Carlucci, L.; Ciani, G.; Proserpio, D. M.; Sironi, A. *J. Mater. Chem.* **1997**, *7*, 127. (b) Carlucci, L.; Ciani, G.; von Gudenberg, D. W.; Proserpio, D. M.; Sironi, A. *Chem. Commun.* **1997**, 631. (c) Carlucci, L.; Ciani, G.; Proserpio, D. M.; Rizzato, S. *J. Solid State Chem.* **2000**, *152*, 211. (d) Tong, M.-L.; Zheng, S.-L.; Chen, X.-M. *Chem.—Eur. J.* **2000**, *6*, 3729. (e) Bu, W.-M.; Ye, L.; Fan, Y.-G. *Chem. Lett.* **2000**, 152. (f) Moulton, B.; Lu, J.; Zaworotko, M. J. *J. Am. Chem. Soc.* **2001**, *123*, 9224. (g) Zheng, S.-L.; Tong, M.-L.; Tan, S.-D.; Wang, Y.; Shi, J.-X.; Tong, Y.-X.; Lee, H. K.; Chen, X.-M. *Organometallics* **2001**, *20*, 5319. (h) Zheng, S.-L.; Zhang, J.-P.; Chen, X.-M.; Ng, S.-W. *J. Solid State Chem.* **2003**, *172*, 45. (i) Konar, S.; Mukherjee, P. S.; Drew, M. G. B.; Ribas, J.; Chaudhuri, N. R. *Inorg. Chem.* **2003**, *42*, 2545. (j) Fang, Q.; Zhu, G.; Xue, M.; Sun, J.; Wei, Y.; Qiu, S.; Xu, R. *Angew. Chem., Int. Ed.* **2005**, *44*, 3845.

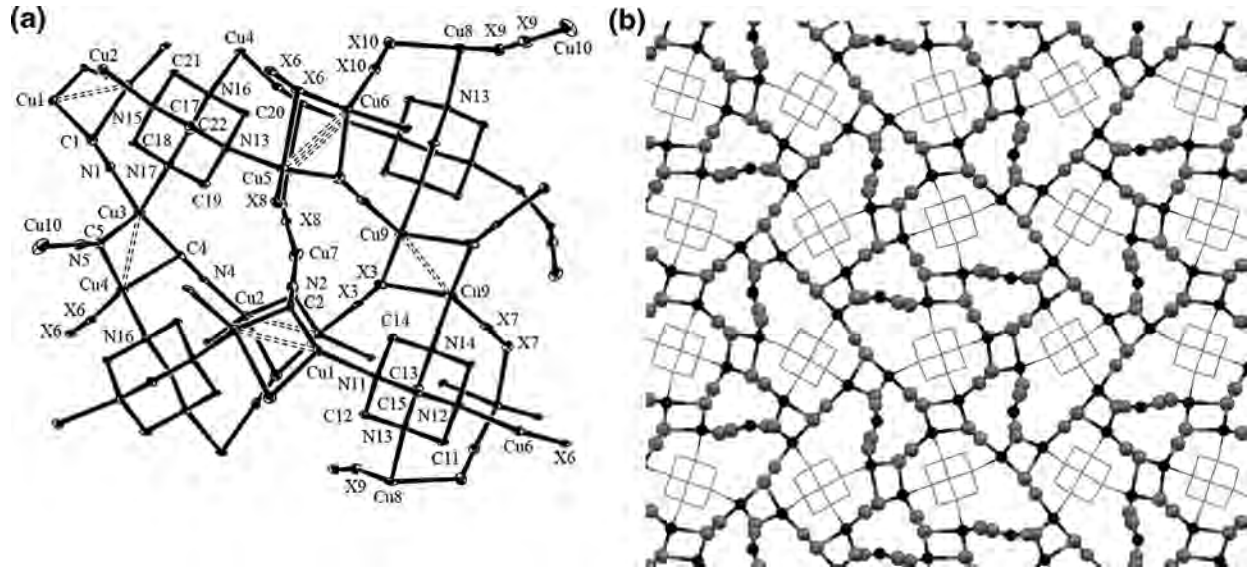

Figure 10. X-ray crystal structure of $(CuCN)_5(HMTA)$, **9c**. Hydrogen atoms omitted for clarity. (a) Thermal ellipsoid view (50%). All Cu···Cu interactions are shown with dashed bonds. (b) Projection down crystallographic *a* axis. Cu···Cu interactions are not shown.

Section; the TGA traces are included in the Supporting Information. Decomposition temperatures for the piperazine complexes are generally modest, typically commencing around 150−180 °C. However, the HMTA materials exhibit high thermal stability. It is noteworthy that increasing the number of metal centers bound to HMTA produces denser, more highly cross-linked networks, which show increasing decomposition temperature in TGA results. Thus, **9a** (bidentate), **9b** (tridentate), and **9c** (tetradentate) begin to lose HMTA at 215, 240, and 290 °C, respectively. In all cases, the multistep decomposition of CuCN began at about 400 °C. Relatively copper-deficient networks of BzPip and Ph_2CHPip and HMTA showed plateaus prior to the ultimate formation of CuCN. Based upon TGA mass percent values, transformation sequences (1) through (5) are strongly indicated:

$$(CuCN)_3(BzPip)_2(\mathbf{6a}) \rightarrow (CuCN)_3(BzPip) \rightarrow CuCN \quad (1)$$

$$(CuCN)_5(BzPip)_2(\mathbf{6b}) \rightarrow (CuCN)_4(BzPip)(\mathbf{6d}) \rightarrow CuCN \quad (2)$$

$$(CuCN)(Ph_2CHPip)(\mathbf{8a}) \rightarrow (CuCN)_2(Ph_2CHPip)(\mathbf{8b}) \rightarrow CuCN \quad (3)$$

$$(CuCN)_3(HMTA)_2(\mathbf{9a}) \rightarrow (CuCN)_5(HMTA)(\mathbf{9c}) \rightarrow CuCN \quad (4)$$

$$(CuCN)_5(HMTA)_2(\mathbf{9b}) \rightarrow (CuCN)_5(HMTA)(\mathbf{9c}) \rightarrow CuCN \quad (5)$$

The most interesting decomposition patterns arise in the diverse CuCN−BzPip system. All suggested intermediates in the CuCN−BzPip sequence, except $(CuCN)_3(BzPip)$, represent known compositions. However, it is intriguing that **6a** and **6b** appear to progress through different intermediate stoichiometries during their decomposition reactions.

Infrared Spectroscopy. Infrared analysis of the powder samples revealed the expected intense cyanide stretching bands, occurring in the 2075−2162 cm^{-1} range. The $(CuCN)_2L$ species, **1a**, **3a**, **7**, and **8b** were found to show only a single C≡N band. This fact is consistent with the relatively simple structures of these networks. However, the other network that showed a single cyanide band, **1b**, had the most complex structure, with 20 separate cyanide groups. It is generally recognized that an inverse correlation exists between C≡N stretching frequency and Cu−X (X = C/N) bond length.[20] Thus in our previous study, it was noted that in each case where weak cyano bridging produced a long Cu−X interaction of >2.0 Å, a band of <2100 $cm^{-1}$was present in the IR spectrum.[1] In the present study, only **6c**, **9b** and **9c** exhibited C≡N stretches of <2100 cm^{-1}. The structure of **6c** is as of yet unknown. However, both **9b** and **9c** have long Cu−X distances as part of triply bridging cyanide arrangements. Although **1a** shows cyanide bridging of four metal centers, it lacks a low frequency C≡N stretch because all Cu−X bond lengths in **1a** are relatively short.[7]

Luminescence Spectroscopy. Solid-state luminescence measurements were carried out at ambient temperature using powder samples. Selected samples were examined for luminescence at 77 and 4 K. The results are summarized in Table 4 and several traces are presented in Figures 11–13. Additional spectra are included in the Supporting Information. As shown in part a of Figure 11, copper(I) cyanide itself shows solid-state luminescence behavior, having a broad excitation feature with peaks at about 288, 307, and 345 nm. A fairly sharp emission peak centered at 392 nm moves to 412 nm at 77 K. Because this peak lies at the UV−vis border, CuCN shows a faint purple emission under a black-light. Our previous studies of CuCN networks with diimine L ligands indicated substantial to complete quenching of this luminescence upon network formation. In stark contrast to these previous results, the networks based on the diamine ligands showed a variety of luminescence intensities, ranging from almost no response above baseline to intensity comparable to that of CuCN itself.

Table 4. Luminescence results

complex[a]	*T*, K	excitation λ_{max}, nm	emission λ_{max}, nm (color)	Stokes shift, cm^{-1}[b]
CuCN	298	285, 309, 350	391 (purple)	2996
	77	288, 307, 345	412 (purple)	
$(CuCN)_2(Pip)$, **1a**	298	282, 308	458 (blue)	10 634
	77		(blue)	
$(CuCN)_{20}(Pip)_7$, **1b**	298	286, 322, 345	443 (blue)	6413
	77	345	443 (blue)	
$(CuCN)_7(MePip)_2$, **2**	298	284, 340	445 (blue)	6940
	77	340	445 (blue)	
$(CuCN)_2(Me_2Pip)$, **3a**	298	281, 332	485 (yellow-green)	9501
	77		(blue)	
$(CuCN)_4(Me_2Pip)$, **3b**	298	284, 328	487 (green)	9954
	77	325	412, 460 (blue)	
$(CuCN)_7(EtPip)_2$, **4**	298	284, 335	445 (blue)	7379
	77	310, 335	449 (blue)	
	4	312, 341	450	
$(CuCN)_4(Et_2Pip)$, **5**	298	284, 315	436 (purple)	8810
	77	307	415 (purple)	
$(CuCN)(Ph_2CHPip)$, **8a**	298	282, 317	484 (yellow-green)	10 885
	77		(blue)	
$(CuCN)_2(Ph_2CHPip)$, **8b**	298	281, 321	443, 575 (orange)	8580
	77	323	442, 592 (purple)	
	4	325	377, 444	
$(CuCN)_3(HMTA)_2$, **9a**	298	281, 304	390, 475, 505 (blue-green)	11 842
	77		(purple)	
$(CuCN)_5(HMTA)_2$, **9b**	298	285, 302	470, 510 (yellow)	11836
	77		(blue)	
$(CuCN)_5(HMTA)$, **9c**	298	282, 304	417, 522 (yellow-green)	8914
	77	304	417, 522 (blue)	
	4	295	416, 451	

[a] Other complexes had no luminescence response. [b] Calculated between longest excitation λ_{max} and shortest emission λ_{max}.

All of the network complexes, except **6a**−**d** and **7**, were luminescent at room temperature. In all cases broad excitation features, not significantly different from those of CuCN, were seen in the 250−350 nm range. As many as two emission bands were observed. A high energy (HE) band in the 435−450 nm range was noted for all luminescent products. This band is probably analogous to the CuCN 392 nm emission band. For some compounds a second low energy (LE) band was also noted in the 470−575 nm range. Complexes lacking the LE band (**1a**, **1b**, **2**, **4**, and **5**) showed intense blue luminescence, whereas those having both HE and LE bands (**3a**, **3b**, **8a**, **8b**, **9a**, **9b**, and **9c**) displayed luminescence of varying intensity ranging from green to orange at ambient temperature. For all species except **8b** and **9a**−**c**, the LE band overlapped the HE band, resulting in a single broad emission feature.

Low-temperature luminescence studies (Table 4, Figures 11–13) revealed significant thermochromism in some cases. As noted above, the sharp CuCN emission band moves from 391 nm at ambient temperature to 412 nm at 77 K. For the network complexes, cooling to 77 K usually had no effect on excitation or HE emission wavelength. Several compounds lacking LE bands (**1b**, **2**, **4**, and **5**) were examined at reduced temperature. They showed a simple increase in intensity and no change in λ_{max}. The behavior of **2** is representative and is shown in part b of Figure 11. The only exception was **5**, for which HE λ_{max} fell slightly, from 436 to 415 nm. In some cases, such as **4** (part c of Figure 11), careful examination of the luminescence behavior at 77 K revealed that the broad excitation band is actually composed of three peaks (280, 320, and 354 nm) and the emission band is composed of two peaks (412 and 449 nm). The strongest excitation and emission peaks for **4** at 320 and 449 nm are coupled, as are the somewhat weaker intensity peaks at 354 and 412 nm. Similar behavior was noted for **3b** (Supporting Information). Because **3b** and **4** do not show separate LE features, it is not clear whether these closely spaced emission peaks are two components of the HE band or whether they represent the HE and LE bands.

Thermochromism. The LE band showed thermochromic behavior, most strikingly so for **8b** and **9c** which have widely separated HE and LE bands (443 and 575 nm for **8b** and 417 and 522 nm for **9c**). Variable-temperature spectra and photographs of these compounds are shown Figures 12and 13. **3a**, **3b**, **8a**, **9a**, and **9b** are also thermochromic, shifting from green or yellow-green to blue emission upon cooling to 77 K (Supporting Information for additional photos). The marked color change in **8b** and **9c** at low temperature is due to significant increase in intensity of the HE band and at least partial disappearance of the LE feature. In the case of **9c**, a new shoulder at 451 nm becomes apparent at 4 K. It is suggested that this represents splitting of the HE band (as is noted for **3b** and **4**, e.g.), rather than persistence of the LE band.

Luminescence Interpretation. Luminescence behavior in Cu(I) complexes (other than Cu_4X_4 and related clusters) is commonly attributed to a Cu $d^{10} \rightarrow d^9s^1$ or d^9p^1 metal-centered (MC) transition;[23] however, when unsaturated ligands are present metal-to-ligand charge transfer (MLCT) can also be invoked.[6k,24] Copper−copper interactions of <3 Å are absent in both the low- and high-temperature forms of CuCN, ruling out metal-to-metal charge transfer as a likely source of luminescence.[18] Preliminary data from a DFT study in our laboratory using *Gaussian98* suggests that the CuCN

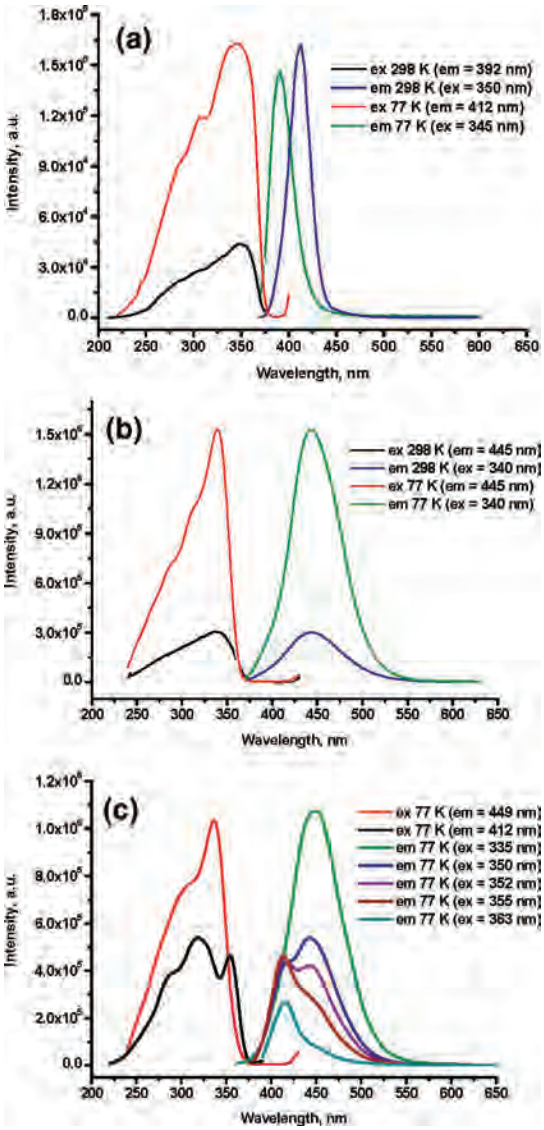

Figure 11. Luminescence spectra: (a) CuCN at 298 and 77 K; (b) **2**, $(CuCN)_7(MePip)_2$ at 298 and 77 K; (c) **4**, $(CuCN)_7(EtPip)_2$ at 77 K.

HOMO is of metal $3dz^2/4s$ character, whereas the LUMO combines metal 4p and π^*_{CN} contributions. This would indicate that a combination of MC and MLCT underlies the CuCN HE band. Turning attention to CuCN−L complexes, we have previously noted that the excitation spectra of **1b** appears very similar to that of CuCN.[2] This now appears to be the case for all of the luminescent complexes reported herein. When excitation fine structure is observable, as is the case for **4** (part c of Figure 11), the observed peaks (280, 320, and 354 nm) are very similar in position and relative intensity to those of CuCN (288, 307, and 345 nm). Therefore, it seems safe to propose that the photophysics of CuCN are not significantly altered upon network expansion with piperazines. Moving from CuCN to the CuCN−piperazine network complexes, there is an apparent emission red shift in this HE band of about 50 nm. However, careful examination of the spectra reveals that in at least some of the networks the HE emission band is composed of a pair of features that become more readily discernible at low temperature (part c of Figure 11). One of these emission

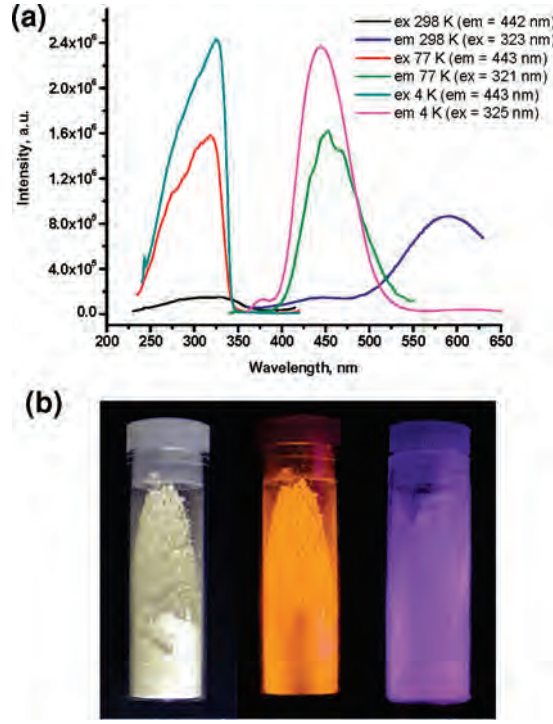

Figure 12. Luminescence of **8b**, $(CuCN)_2(Ph_2CHPip)$: a) spectra at 298, 77 and 4 K. b) photos (left to right) room light/298 K, UV light/298 K, UV light/77 K.

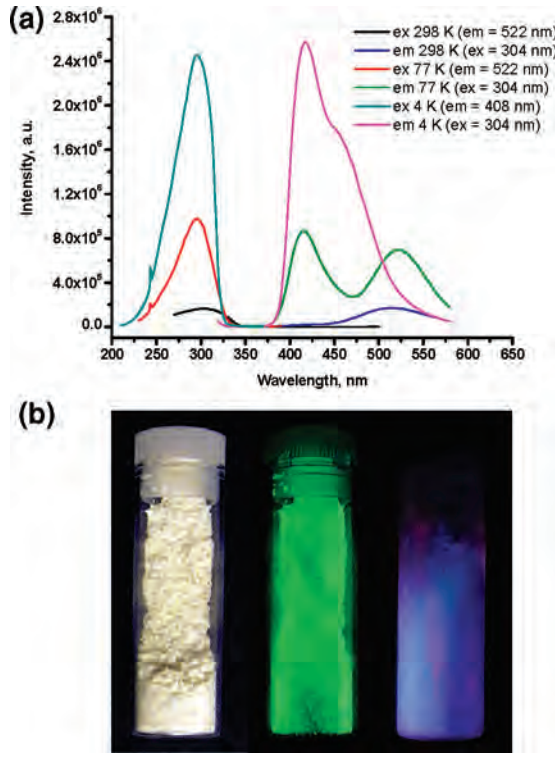

Figure 13. Luminescence of **9c**, $(CuCN)_5(HMTA)$:)a) spectra at 298, 77 and 4 K; (b) photos (left to right) room light/298 K, UV light/298 K, UV light/77 K.

features is identical to that of CuCN (λ_{max} = 412 nm), and the second shows a red shift to about 440−460 nm. The 412 nm band is more prominent when excitation is carried out at longer wavelengths. We suggest that this 412 nm band is the result of the 2-coordinate copper centers that form the

CuCN chains (the B sublattice), which are present in all of the networks having >2:1 CuCN/L stoichiometry. If this explanation is correct, then the 440−460 nm emission would reasonably be associated with the 3-coordinate copper centers in the A sublattice. Whereas the 440−460 nm peak is observable in all the luminescent complexes reported herein, the 412 peak is discernible only in a few cases, such as **3b** and **4**, both of which have been confirmed by X-ray as containing 2-coordinate copper centers.

Some of the complexes described herein show a LE feature in addition to the pervasive HE band. The two bands show markedly different temperature behavior. Whereas the HE band consistently increases in relative intensity when the temperature is lowered to 77 K, the LE band is diminished in intensity under these conditions. **8b** and **9c** in particular have relatively long wavelength LE bands that are strongly temperature dependent. Low-temperature luminescence spectroscopy results have shown that the **8b** and **9c** LE bands disappear completely at reduced temperature (parts d and e of Figure 11). This change in the relative intensity of the HE and LE bands with temperature is due to energy transfer between the high-energy sublattices and low-energy sublattices. At 77 K, the barrier to energy transfer is larger than kT and very little energy transfer occurs, but at 298 K energy transfer occurs easily and the LE band is observed. The results reported herein are similar to those we have reported for metal dicyanides such as $K[Au_xAg_{1-x}(CN)_2]$, as well as for $K[Au(CN)_2]$ and $K[Ag(CN)_2]$ both pure and doped as impurities in KCl.[25]

It is remarkable that the complexes of Me_2Pip (**3a** and **3b**) show both HE and LE bands, giving rise to yellow to green luminescence, whereas those of Pip, MePip, EtPip, and Et_2Pip produce blue luminescent materials (HE band only). This is the case in spite of the fact that **3b** (Me_2Pip) and **5** (Et_2Pip) are structurally similar to one another.

In Table 4, we tabulate the various Stokes shift values by taking the difference between the longest wavelength excitation band and the HE emission at room temperature. When the Stokes shift is of the order of 8000 cm^{-1} or greater, the HE band is most likely a MLCT transition because there is a bond order difference between the HOMO and LUMO states. However, when the Stokes shift is much smaller, then the HE emission band is most likely a MC transition. This is because the bond order difference of the HOMO and the LUMO states should be small because both the HOMO and LUMO states are of the same metal origin.

The absence of measurable luminescence behavior in the BzPip and Bz_2Pip species is most readily ascribed to electronic coupling in the excited state to π^* orbitals in the benzyl groups, facilitating nonradiative relaxation. However, it should be noted that the mere presence of aromatic features is not enough to ensure quenching of the copper-based luminescence in these networks. Results for **8a** and **8b** and preliminary results with *N*-phenylpiperazine show luminescent products. A word is also in order with regard to Cu···Cu interactions and luminescence. As stated above, CuCN itself is luminescent and yet lacks such interactions. Although such close contacts are seen in many of networks reported herein, they are probably not connected with the luminescence seen. This assertion is supported by the fact that CuCN and its amine networks show related photophysical behavior and also by the nearly identical behavior of **3a** and **3b**, the former of which lacks CuCN threading and the associated Cu···Cu interactions.

Conclusion

In summary, we have described a large number of very stable metal−organic networks that combine CuCN and L = various substituted piperazines or HTMA. The products are formed in simple aqueous reactions. A very common structural theme in these networks is the hexagonally tiled (6,3) sheet composed of CuCN chains cross-linked by L giving rise to 2:1 CuCN/L stoichiometry. Additional CuCN chains can be incorporated by threading through the hexagonal channels in the (6,3) sheets, resulting in 7:2 or 4:1 stoichiometry. Bond angles for both 2- and 3-coordinate copper are highly variable. The orientation of the piperazine ligands tends to favor axial coordination of copper, but exceptions do occur. The bulky Ph_2CHPip ligand remains monodentate, producing a very unusual structure in which a CuCN chain is decorated with CNCuL units. The HMTA unit can be bi, tri, or tetradentate in CuCN complexes, leading to extensive $Cu_2(CN)_2$ dimer formation in the latter two cases.

Networks lacking benzyl groups show moderate to strong photoluminescence, which is probably associated with MLCT transitions. Networks containing Pip, MePip, EtPip, and Et_2Pip show strong blue luminescence, which results from an apparent combination of a sharp CuCN-like emission feature and a broader emission band that is probably associated with 3-coordinate copper centers. This HE band intensifies at lower temperature. In complexes containing Me_2Pip, Ph_2CHPip, and HMTA, a LE band has also been identified. Although its origin is unclear, its intensity is sharply diminished at reduced temperature, resulting in interesting thermochromic behavior.

Acknowledgment. Grateful acknowledgement is made to the donors of the American Chemical Society Petroleum Research Fund (44891-B3). We also acknowledge a Howard Hughes Medical Institute grant through the Undergraduate Biological Sciences Education Program to the College of

(23) (a) Ford, P. C.; Cariati, E.; Bourassa, J. *Chem. Rev.* **1999**, *99*, 3625, and references cited therein. (b) Vega, A.; Saillard, J.-Y. *Inorg. Chem.* **2004**, *43*, 4012. (c) Lin, Y.-Y.; Li, S.-W.; Che, C.-M.; Fu, W.-F.; Zhou, Z.-Y.; Zhu, N. *Inorg. Chem.* **2005**, *44*, 1511. (d) Bi, M.; Li, G.; Zou, Y.; Shi, Z.; Feng, S. *Inorg. Chem.* **2007**, *46*, 604.

(24) (a) Näther, C.; Greve, J.; Jess, I.; Wickleder, C. *Solid State Sci.* **2003**, *5*, 1167. (b) Liu, X.; Guo, G.-C.; Wu, A.-Q.; Cai, L.-Z.; Huang, J.-S. *Inorg. Chem.* **2005**, *44*, 4282. (c) Araki, H.; Tsuge, K.; Sasaki, Y.; Ishizaka, S.; Kitamura, N. *Inorg. Chem.* **2005**, *44*, 9667. (d) Araki, H.; Tsuge, K.; Sasaki, Y.; Ishizaka, S.; Kitamura, N. *Inorg. Chem.* **2007**, *46*, 10032.

(25) (a) Omary, M. A.; Hall, D. R.; Shankle, G. E.; Siemiarczuk, A.; Patterson, H. H. *J. Phys. Chem. B* **1999**, *103*, 3845. (b) Rawashdeh-Omary, M. A.; Omary, M. A.; Shankle, G. E.; Patterson, H. H. *J. Phys. Chem. B* **2000**, *104*, 6143. (c) Hettiarachchi, S. R.; Schaefer, R. L.; Yson, R. L.; Staples, R. J.; Herbst-Irmer, R.; Patterson, H. H. *Inorg. Chem.* **2007**, *46*, 6997.

William and Mary. The research at the University of Maine was supported by the National Science Foundation. We are indebted to NSF (CHE-0443345) and the College of William and Mary for the purchase of X-ray equipment.

Supporting Information Available: (1) Full details of the crystal structure determinations for **1b**, **2**, **3b**, **4**, **5**, **6a**, **6d**, **7**, **8b**, **9b** and **9c** in CIF format and tables of crystal data, atomic coordinates, bond lengths and angles, and anisotropic displacement parameters; (2) X-ray powder patterns (experimental and calculated) for all structurally characterized compounds; (3) TGA traces for all compounds; (4) additional luminescence spectra for all luminescent compounds; and (5) luminescence photos for all luminescent compounds. This material is available free of charge via the Internet at http://pubs.acs.org.

IC8005184